Laboratório de Implantação Iônica
Instituto de Física - UFRGS

Annual Report 2011

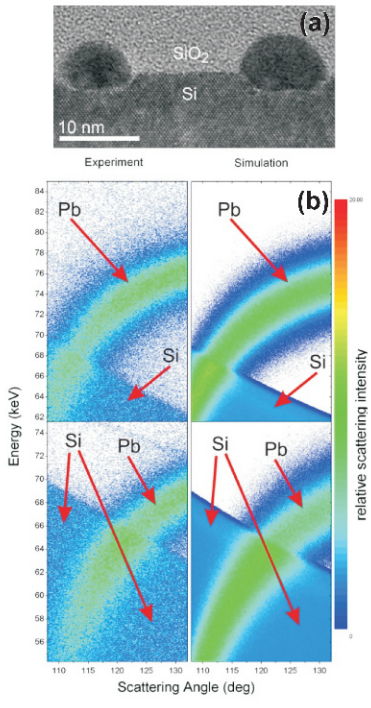

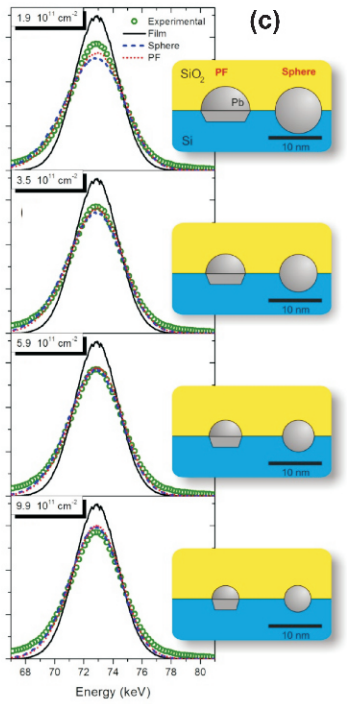

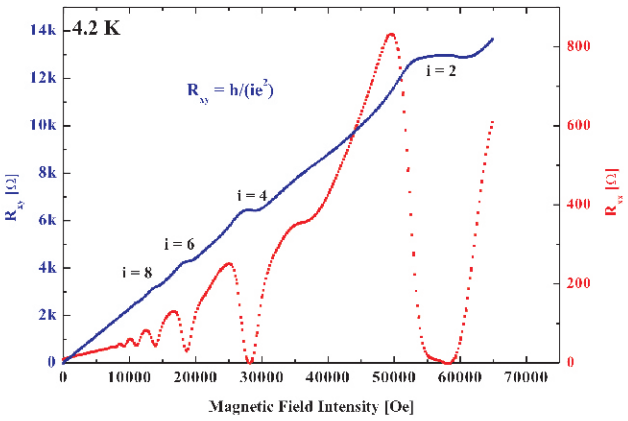

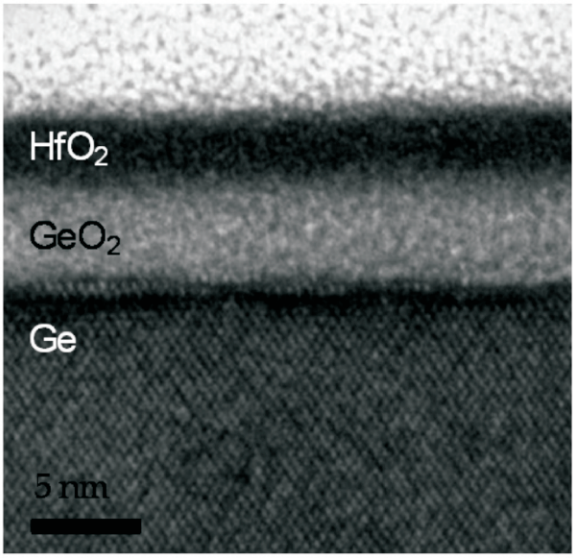

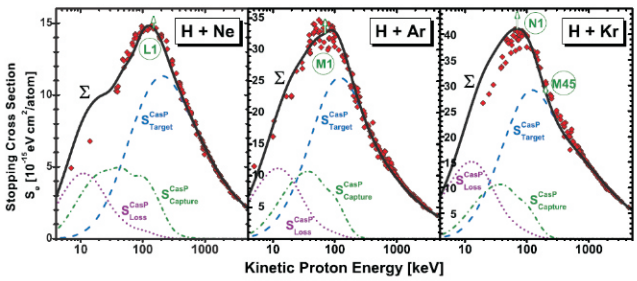

Ion Implantation Laboratory
Institute of Physics - UFRGS
Porto Alegre
Brazil

UFRGS
UNIVERSIDADE FEDERAL DO RIO GRANDE DO SUL

Laboratório de
Implantação Iônica
Instituto de Física - UFRGS

Annual Report 2011

Editors

Pedro Luis Grande

Daniel Lorscheitter Baptista

Raul Carlos Fadanelli Filho

Table of contents

Preface	2
Staff -2011	4
International collaborators	9
Brazilian collaborators	11
Facilities	12
Research Projects	13
Publications of Peer Reviewed articles	66
Conference proceedings	73
Patent	74
Oral contributions and invited talks	75
Books and book chapters	78
Supervision of theses and dissertations	78
Members in int. commitees and in editorial boards of scientific journals	79
Seminars	80
Partners and Projects	83
Funding Agencies	84

Preface

The Ion Implantation Laboratory is an ion beam center at the Institute of Physics (IF) at the Federal University of Rio Grande do Sul (UFRGS), Brazil. The IF-UFRGS is located in the city of Porto Alegre (state of Rio Grande do Sul) and it is ranked as the most important research center of Physics in southern Brazil. The staff of the Institute is composed of 83 Ph.D. researchers divided in two Departments (Physics and Astronomy). Currently, the Institute has around 120 graduate students and is responsible for the Physics courses to approximately 2000 undergraduates of different fields.

The activities on ion beams started in 1981 with the acquisition of a 400 kV particle accelerator (which was modified to 500 kV in 1996). In 1989 an ion implanter of 250 kV was donated by IBM (USA) and is currently dedicated to microelectronic applications. In January 1995 an important upgrade was done with the acquisition of a 3 MV TANDEM accelerator. Both machines provide a wide variety of positive ions in a broad energy range. Several beam lines with different analytical techniques are available to scientists from different fields. The techniques are:

1) **PIXE** (Particle-Induced X-ray Emission): provides elemental concentrations of the order of part per million;
2) **RBS** (Rutherford Backscattering Spectrometry): used for characterization of different structures, including multi-layered targets;
3) **NRA** (Nuclear Reaction Analysis): ideal for profiling and studies of elemental distribution;
4) **Microprobe:** allow the use of techniques like PIXE, RBS and STIM with micrometer beam size;
5) **MEIS** (Medium Energy Ion Scattering): it is a high-resolution RBS technique with isotope-separation capability;
6) **Ion Implantation**: used for modification of materials under controlled parameters.

The infrastructure of the laboratory includes a large variety of charged-particle, X-ray and gamma detectors, modular electronics, ovens and other related equipment. A fully-dedicated workshop allows the maintenance of the laboratory in a regular basis. A general view of the laboratory is shown below, featuring the beam lines of the Tandetron accelerator.

Many researchers from the Ion Implantation Laboratory are also engaged to other labs or facilities from IF-UFRGS. In particular the Laboratory of Microelectronics and the Laboratory of Solid Interfaces and Surfaces are associated laboratories and share many scientific projects.

This is the second issue of the annual report. The scientific activities described here show the growing of the Laboratory. In the last two years (2010/2012) many young professors have joined our laboratory. In addition, in 2011 we have organized the 20th edition of the International Conference on Ion Beam Analysis (IBA), in Itapema, Santa Catarina. The successful organization of this conference, the largest conference on ion beam analysis of the world, among other conferences we have organized so far, reflects the progression of our Laboratory which I hope will continue in the following years.

Pedro L. Grande
Head of Ion Implantation Laboratory

Staff - 2011

Permanent

Fernando Claudio Zawislak, PhD. (IF, UFRGS, 1967) - Founder and Group leader between 1980 and 2008

Moni Behar, PhD. (UBA, ARGENTINA, 1970) – Accelerators coordinator between 1982 and 2009

Israel Jacob Rabin Baumvol, PhD. (IF, UFRGS, 1977)

Livio Amaral, PhD. (IF, UFRGS, 1982)

Paulo Fernando Papaleo Fichtner, PhD. (IF, UFRGS, 1987)

Pedro Luís Grande, PhD. (IF, UFRGS, 1989) - Group leader since 2009.

Johnny Ferraz Dias, PhD. (UG, BELGIUM, 1994) – Accelerators coordinator since 2010.

Henri Ivanov Boudinov , PhD. (IE-BAN, BULGARY, 1991)

Fernanda Chiarello Stedile, PhD. (IQ, UFRGS, 1994)

Ricardo Meurer Papaléo, PhD. (U.UPPSALA, SWEDEN, 1996) - PUC-RS

Rogério Luis Maltez, PhD. (IF, UFRGS, 1997)

Claudio Radtke,PhD. (IF, UFRGS, 2003)

Cristiano Krug, PhD. (IF, UFRGS, 2003)

Gustavo de Medeiros Azevedo, PhD. (IF, UFRGS, 2000)

Daniel Lorscheitter Baptista, PhD. (IF, UFRGS, 2003)

Gabriel Viera Soares, PhD. (IF, UFRGS, 2008)

Raul Carlos Fadanelli Filho, PhD. (IF, UFRGS, 2005)

Rafael Peretti Pezzi, PhD. (IF, UFRGS, 2009)

Leandro Langie Araujo, PhD. (IF, UFRGS, 2004)

Raquel Giulian, PhD. (RSPE, ANU, AUSTRALIA, 2009)

Agenor Hentz da Silva Jr., PhD. (UFRGS, BRAZIL, 2007)

Technicians

Agostinho A. Bulla, Electrical Engineer responsible for the accelerators

Zacarias E. Fabrim, Mechanical Engineer responsible for the clean-room

Clodomiro F. Castello, Accelerator support and operation

Paulo R. Borba, Accelerator support and operation

Paulo Kovalik, Workshop

Éder Bidinotto Brito, Sample preparation and clean-room assistant

Postdocs

Artur V. P. Coelho

Felipe Kremer

Giovani Pesenti

Karen P. Bastos

Maria Lucia Yoneama

Paulo L. Franzen

Rodrigo Palmieri

Samir Shubeita

Uilson S. Sias

PhD Students

Ataídes Martins Botelho Neto

Augusto A. D. de Mattos

Carla Eliete Iochims dos Santos

Caroline Lisevski

Cláudia Telles de Souza

Cristiane Marin

Dario F. Sanchez

Deise Schafer

PhD Students (continued)

Eliasibe Luis de Souza

Elis Moura Stori

Felipe Bregolin

Flávia P. Luce

João Wagner Lopes de Oliveira

Liana Appel Boufleur

Luiz Acauan

Maurício Sortica

Nicolau Molina Bom

Rafael Otoniel

Ramon Ferreira Jr.

Roberto Moreno de Souza Reis

Silma Alberton Corrêa

Zacarias Eduardo Fabrim

MSc students

Aline Taís da Rosa

André Cauduro

Antônio de Mattos

Eduardo Pitthan Filho

Gabriel Marmitt

Guilherme Sombrio

Ivan Rodrigo Kaufmann

Ludmar Matos

Luiz Gustavo Barbosa

Matheus Adam

Masahiro Hatori

Rafaela Debastiani

International collaborators

L. Thome, Orsay, France.

F. Garrido, Orsay, France.

W. Skorupa Rossendorf, Germany.

L. Rebohle, Rossendeorf, Germany.

I. Abril, University of Alicant, Spain

F. Garcia- Molina University of Murcia, Spain.

G. Garcia Bermudez, Lab. Tandar CNEA, Argentina.

N. Arista CAB, CNEA, Argentina.

S. Suarez CAB, CNEA, Argentina.

G. Lucovsky, NCSU, EUA.

J.M.J. Lopes, PDI, Germany.

L. Feldman, Rutgers University, U.S.A.

A. Agarwal,Cree Inc., U.S.A.

A. Lelis, Army Research Lab., U.S.A.

S. Dimitrijev, Griffith University, Austrália.

G. Schiwietz, Helmholtz-Zentrum Berlin, Germany.

J. Kennedy, GNS, New Zealand.

H. Rothard, GANIL, France.

C. D. Denton, University of Alicant, Spain.

D. K. Ferry, Arizona State University, U.S.A.

V. Mittin, State University of New York at Buffalo, U.S.A.

M.C. Ridgway, The Australian National University, Australia.

H.G. Rubahn, NanoSYD, Sonderborg, Denmark.

Z. Liliental-Weber, LBNL, U.S.A.

C. Trautmann, GSI, Darmstadt, Germany.

F. Aumayr,Vienna University of Technology, Vienna, Austria.

E. Oliviero, University of Paris-Sud (Orsay), France.

J-F Barbot, University of Poitiers, France.

M. F. Beaufort,University of Poitiers, France.

S. Reboh, Laboratoire d'électronique des technologies de l'information, Grenoble, France.

Brazilian collaborators

L.M. Nagamine, USP, São Paulo - SP

R.P. Menezes, PUC, Rio de Janeiro - RJ

E.F. da Silveira, PUC, Rio de Janeiro - RJ

L.S. Farenzena, UFSC, Florianópolis - SC

G. Machado, CETENE, Recife - PE

L. Miotti, Caxias do Sul - RS

J. Geshev, UFRGS, Porto Alegre - RS

L.G. Pereira, UFRGS, Porto Alegre - RS

M. Schiavon, UFSJ, São João del-Rei - MG

U.S. Sias, IFSul, Pelotas - RS

E.F. da Silva Jr., UFPE, Recife - PE

A.A. Pasa, UFSC, Florianópolis - SC

I. Hummelgen, UFPR, Curitiba - PR

J.W. Swart, CTI, Campinas - SP

J.A. Diniz, UNICAMP, Campinas - SP

G. Kellermann, UFPR, Curitiba - PR

A. Malachias, UFMG, Belo Horizonte - MG

T. Marcondes, CBPF, Rio de Janeiro - RJ

R.L. Sommer, CBPF, Rio de Janeiro - RJ

L. Sampaio, CBPF, Rio de Janeiro - RJ

V.P. Mammama, CTI, Campinas - SP

L. F. Schelp, UFSM, Santa Maria - RS

M. Carara, UFSM, Santa Maria - RS

L. S. Dorneles, UFSM, Santa Maria - RS

Facilities

Besides the accelerators the laboratory has the following facilities

a) Photoluminesce laboratory

b) Cleanroom

c) Furnaces, ovens and reactor chambers

Tandetron accelerator

500 kV accelerator

250 kV accelerator

Furnaces and reactors

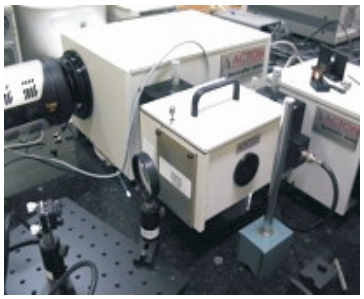

Optical characterization

Clean room

Workshop

Support room

Research Projects

Sharp Transition from Normal to Abnormal Grain Growth of Nanostructured Al Thin Films

F. C. Zawislak

Introduction

Thin films structural features such as grain size, size distribution, texture and morphology can significantly influence the desired performance in many applications. For example, metallic interconnections of microelectronic devices with large, defect-free grains are typically more resistant against electromigration failures than small grain size counterparts. Generally the deposited films have a columnar grain structure presenting a large thermal stability. In this contribution we report on a new concept of multi-step deposition were columnar grains are avoided and a mosaic-like nanocrystalline grain structure with small size dispersion is obtained.

Results

Nanocrystalline Al thin films (180 nm thick) were deposited via magnetron sputtering technique, using a multi-step deposition process. The resulting films have a mosaic-like structure of small grains with characteristic mean diameter of 30 nm. The evolution of the grain size distribution was investigated as function of annealing in vacuum for temperatures from 300 to 525 °C, using transmission electron microscopy and x-ray diffraction techniques. For temperatures in the range of $300 \leq T \leq 462$ °C, the film grains present a 3-D regular growth behavior, up to the diameter sizes of ≈ 50 nm. In the narrow 462 - 475 °C temperature range a rather sharp transition from normal to abnormal grain growth occurs. For $T > 475$ °C the grains extend to the film thickness and present mean lateral dimensions of 1 m. The observed phenomenon is discussed in terms of a synergetic grain boundary mobility effect caused by the initial nanogranular grain boundary morphology. The micrographs of fig 1 show the grain growth evolution of the columnar and of layered mosaic-like films as function of the annealing temperature.

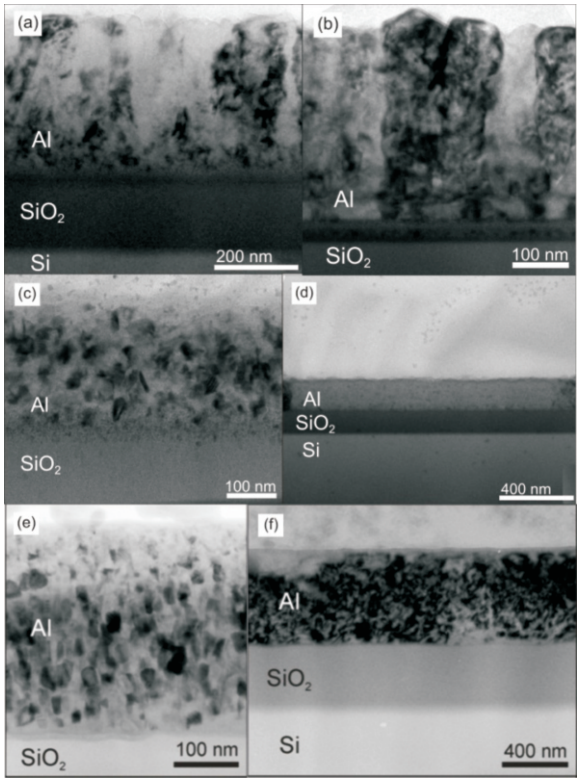

Figure 1 *Cross-section TEM micrographs, showing the microstructural evolution of the columnar and of the four and eight layered mosaic-like films before and after annealing at 500 °C/1h. The columnar structure obtained in the as-deposited film (a) did not change due to the annealing (b). In contrast, the annealing produced dramatic changes of the layered films. The fine grain structure of the as-deposited 4-layered (c) and 8-layered (e) films evolved to large grains, (d) and (f) respectively, after annealing.*

Research outlook

The extension of this work to investigate the electromigration characteristics of other interconnects like Cu, Ag and CuAg and CuAl alloys, will be the subject of further studies. These studies can be performed in collaboration with the local microelectronic device industry.

Publications

[1] F.P. Luce, P.F.P. Fichtner, L.F. Schelp and F.C. Zawislak: Measurments of Al thin films on SiO_2/Si substrate, Mat. Res. Soc. Symp. Proc. vol. 1150 (2009).

[2] F.P. Luce, S. Reboh, Z.E. Fabrin, G. Feldmann, L.F. Schelp, C.S. Camacho, P.F.P. Fichtner and F.C. Zawislak: Sharp Transition from Normal to Abnormal Grain Growth of Nanostructured Al Films, submitted to Scripta Materialia.

Proliferation behavior of fibroblasts on ion beam modified polystyrene

C. Arbeitman, I. Ibañez, H. Ascolani, G. García Bermúdez, M. Behar

Introduction

Ion beam irradiation is a well known means to change the physico-chemical properties of polymers, and induced bio and citocompatibility in controlled conditions and in selected areas of surface. We previously reported that changes in irradiated polymer affect on the initial adhesion of NIH 3T3 fibroblasts [1]. However, the enhancement of cell adhesion on a modified substrate does not mean that the surface is adequate for functional cells. The purpose of the present work is to continue the study in order to determine proliferation and changes in cytoskeleton and cell morphology on substrates as a function of different irradiations parameters. X-ray photoelectron spectroscopy (XPS) was used to determine the changes in the functional groups of the polymeric materials after irradiation. The discussion of the results was based on an analysis of the physicochemical changes induced on the surface.

Results

We observed that the cell evolution is related to filopodia behavior, and changes in cell shape influences proliferation. Due to the no homogenous distribution of ions hits, the cellular receptors may selectively sensed ion hits with varying degrees of overlap. Then leads to the formation of focal contacts which differ according to the irradiation conditions. The proliferation parameter as a function of ion fluence show the existence of a maximum or optimum value. The enhancement of cell responses is considered in connection with the increase of polar functional groups in the polymer surface.

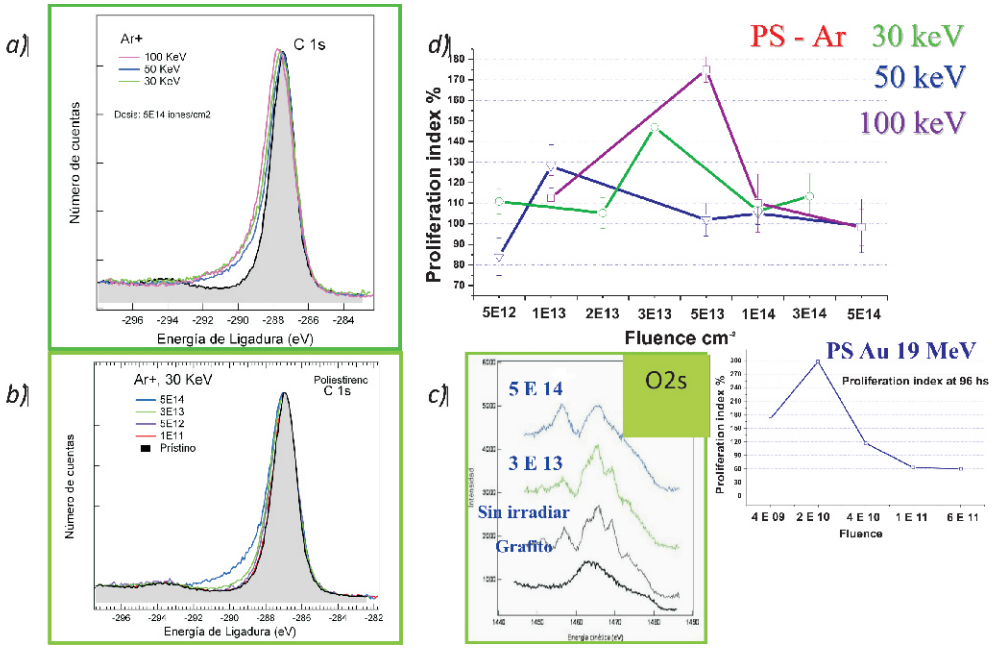

Figure 1 *(a) , (b), (c) XPS: the high resolution scans C1s and O2s peaks. The new intensity in the C1s peak corresponding to the formation of carbon- oxygen bonds. (d) Proliferation index of fibroblasts cultured on PS implanted with Ar ions. (e) PS modified by irradiation with Au at 19 MeV: proliferation index at 96 h.*

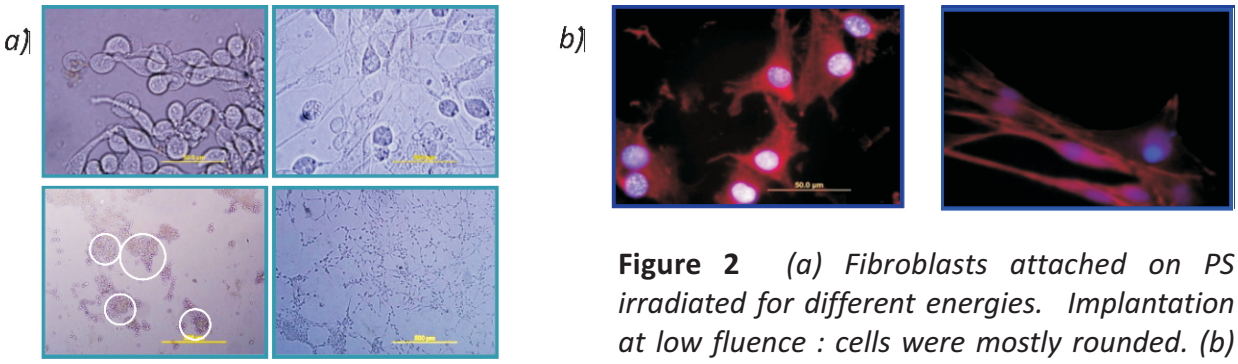

Figure 2 *(a) Fibroblasts attached on PS irradiated for different energies. Implantation at low fluence : cells were mostly rounded. (b) Cytoskeletal organization. Cells stained for F actin.*

Research outlook

Further studies are necessary in order to determine the cellular activities on irradiated polymers.

Publications

[1] C.R. Arbeitman et al. *Irradiation of Polystyrene and Polypropylene to study NIH 3T3 fibroblasts adhesion*. Nucl. Instrum. Meth. Phys. Res. B **268** 3059 (2010).

Experimental and theoretical study of the energy loss of C and O in Zn

R. C. Fadanelli

Introduction

The study of the energy loss of ions in solids is a problem of interest for basic and applied research in many areas, such as ion implantation, radiation damage, and space research.
In this contribution, we show that only the combination of a nonperturbative description, the convolution approximation for swift particles (CasP), with the transport-cross-section–extended-Friedel-sum rule (TCS-EFSR) for the valence electrons leads to a good agreement between experimental and theoretical values for the energy loss of C and O in Zn. Experimental results obtained via RBS measurements are shown as well.

Results

The theoretical work presented here yields two main results
concerning the Zn target:
(1) We determine the limit of applicability of the perturbative shellwise local plasma approximation (SLPA) model, which was successfully applied to projectiles from H to B, and even to C ions but clearly overestimates the O case.
(2) By using the nonperturbative CasP calculations together with the TCS-EFSR method, we obtained a more accurate description of the excitation of bound electrons, which incorporates the property of saturation in the energy loss with increasing Z_1 values.

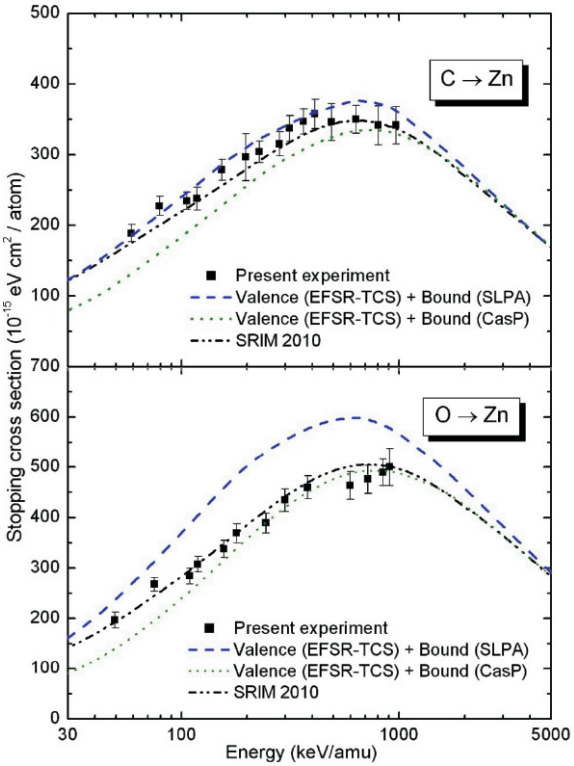

Figure 1 *Stopping cross section as a function of the beam energy for carbon (top) and oxygen (bottom) in Zn. The symbols stand for the experimental results, while the curves stand for the theoretical evaluations performed using EFSR-TCS combined with SLPA (blue dashed line) and CasP (green dotted line).*

Research outlook

The results indicate the necessity of non-perturbative models to describe the energy loss of heavier projectiles in Zn. The previous approach (SLPA and TCS-EFSR) used for H, He, Li, Be e B seems not adequate to describe C and O stoppings.

Publications

[1] E. D. Cantero, C. C. Montanari, M. Behar, R. C. Fadanelli, G. H. Lantschner, J. E. Miraglia, and N. R. Arista, *Experimental and theoretical study of the energy loss of C and O in Zn*. Physical Review A **84** 014902 (2011) .

Depth profiling techniques: how PIXE compares to NRP and MEIS?

J. F. Dias

Introduction

Ion-based techniques like NRP (Nuclear Reaction Profiling) and MEIS (Medium Energy Ion Scattering) are the techniques of choice to profile ultra-thin films in general and oxides in particular.
Other techniques like RBS (Rutherford Backscattering Spectrometry) and PIXE (Particle-Induced X-ray Emission) have been used to study thin films through simultaneous measurements.
The aim of the present work is to check the potentialities of PIXE as an analytical tool for measurement of ultra-thin film thicknesses in the nanometer scale. To that end, several different thin oxide films (HfO_2, $LaScO_3$, $LaAlO_3$ and Al_2O_3) in the range of 2 to 60 nm were grown on crystalline Si. Film thickness measurements using 2.0 and 0.4 MeV proton PIXE, 40 and 200 keV proton MEIS, and 991.9 keV proton NRP were compared.

Results

The overall results are presented in Table 1. For the simple target structures studied in this work, the results indicate that PIXE provides thicknesses compatible to those obtained with NRP and MEIS. However, PIXE analysis proved to be difficult in some cases, particularly when close-by elements with overlapping X-ray peaks are involved. For such cases, MEIS and NRA present clear advantages over PIXE.

Film	Proton Energy (keV)	PIXE Detectors	PIXE (nm)	MEIS (nm)	NRP (nm)	ρ (g/cm³)	ρ* (g/cm³)	ρ** (g/cm³)
HfO_2	2000	Both	2.5 ± 0.4	2.2 ± 0.1	-	9.7	9.7	5.4
$LaScO_3$	2000	Both	9.6 ± 3.0	7.0 ± 0.6	-	4.1	4.0	2.7
$LaAlO_3$	2000	HPGe	8.2 ± 1.9	7.8 ± 0.4	-	4.6	4.3	2.6
Al_2O_3	400	Si(Li)	8.3 ± 2.1	-	8.8 ± 0.4	3.7	4.0	1.9
Al_2O_3	2000	Si(Li)	20.4 ± 6.7	-	8.8 ± 0.4	3.7	4.0	1.9
Al_2O_3	400	Si(Li)	54.2 ± 8.9	-	44.4 ± 2.2	3.7	4.0	1.9
Al_2O_3	2000	Si(Li)	56.9 ± 8.8	-	44.4 ± 2.2	3.7	4.0	1.9

Table 1 *Comparison of film thicknesses obtained by PIXE, MEIS and NRP. The densities were obtained from the simulations carried out with SIMULMEIS and SPACES for the MEIS spectra and NRP excitation curves respectively. The results for HfO_2 and $LaScO_3$ were obtained from experiments were both Si(Li) and HPGe detectors were employed. The proton energies correspond to those employed in the PIXE experiments. In the case of PIXE, the uncertainties represent the standard deviation (at 68 % level) of the PIXE data convoluted with the uncertainties stemming from the fitting procedure of the X-ray spectra. The densities ρ* for HfO_2, $LaScO_3$, $LaAlO_3$ and $Al2O_3$ were measured by other techniques, while ρ** are the values calculated by SRIM code.*

Research outlook

- Analysis of organic tissues, food and beverages using PIXE, RBS, STIM and micro-PIXE;
- Study of plasmon excitations using MEIS;
- Study of Coulomb heating with RBS and PIXE.

Publications

[1] C. E. I. dos Santos, S. M. Shubeita et al., *Depth profiling techniques: how PIXE compares to NRP and MEIS?*, X-Ray Spectrometry **40**, 157 (2011).

Quantum Hall effect as an electrical resistance standard

H. Boudinov

Introduction

In the last ten years an exponential increase of interest in the physics and application of "low-dimensional" semiconductor structures has been observed. From the point of view of electronic transport, this term refers to a system in which the free carriers are confined by potential barriers, so they lose one or more degrees of freedom for motion. In the case of a confining potential well with two-dimensional electron gas (2DEG), the electronic motion will be quantized in the direction of the potential variation, whilst allowing the carriers to move freely in the other two dimensions. We have prepared special sample with very high electron mobility for Quantum Hall Effect (QHE) measurements with high magnetic field. The basic characteristics of the phenomenon have been discussed.

Results

The modulation-doped sample, measured in this work was grown at Research School of Physical Sciences and Engineering, The Australian National University, Canberra, Australia. The sample preparation is described in [1]. Magnetotransport measurements were carried out at Instituto de Fisica, UFRGS on van der Pauw devices with alloyed Au-Ge ohmic contacts in magnetic field up to 6.5 T. Very high transport mobility (m_{eff} = 480000 $cm^2/V\,s$) with a sheet electron density n_s = 2.64x10^{11} cm^{-2} was observed at this temperature.

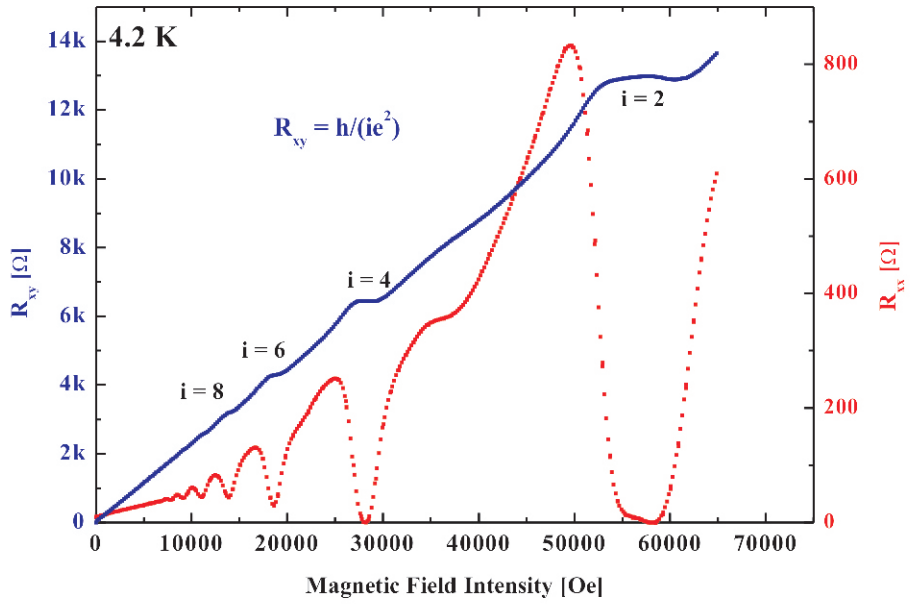

Figure 1 *The R_{xy} and R_{xx} resistance of the modulation doped $Al_{0.3}Ga_{0.7}As/GaAs$ sample, measured at T = 4.2 K in the dark.*

Research outlook

The Quantum Hall Resistivity (QHR) is given by $\rho_{xy} = h/ie^2$, as observed in the experiment. This simple model gives a QHR for certain values of *B* and defines an universal resistance constant: $R_K = h/e^2 = 25812{,}8\,\Omega$. The QHR is an universal constant, independent of host material, device and plateau number. As a consequence, the QHR is used by all the major national metrology institutes as a dc standard for resistance.

Publications

[1] H. Boudinov, M.A.S. Boff, *Quantum Hall Effect as na Electrical Resistance Standard*, ECS Transactions, **39**, 31 (2011).

Effect of Reoxidations and Hydrogen Peroxide in the SiO_2/4H-SiC Interfacial Region

F.C. Stedile

Introduction

Silicon carbide (SiC) is an alternative semiconductor to substitute Si in device applications that require high-power, high-frequency, and/or high-temperature. However, MOS devices based on SiC did not reach the maximum of their potential because of the high interface state density (D_{it}) in the SiO_2/SiC interface. In order to improve the electrical properties of SiC based devices, a better understanding of the SiO_2/SiC region formed and submitted to thermal treatments must be achieved. In this work, different sequential thermal treatments were performed on 4H-SiC polished in both Si and C faces. Their SiO_2/SiC interfacial region thicknesses were determined using the narrow resonance at 151 keV in the cross section curve of the $^{18}O(p,\alpha)^{15}N$ nuclear reaction.

Results

Excitation curves and their respective ^{18}O profiles are shown in figure 1 for samples submitted to sequential treatments: etching in aqueous HF, O_2 bubbled in hot H_2O_2, and thermal oxidation in $^{18}O_2$, repeated a different number of times (samples I, II, and III). In C face samples no major difference is observed in the interfacial region thickness. However, in the case of Si face samples, the most important for devices production, samples that were submitted to more H_2O_2 treatments presented thinner SiO_2/SiC interfacial region thicknesses.

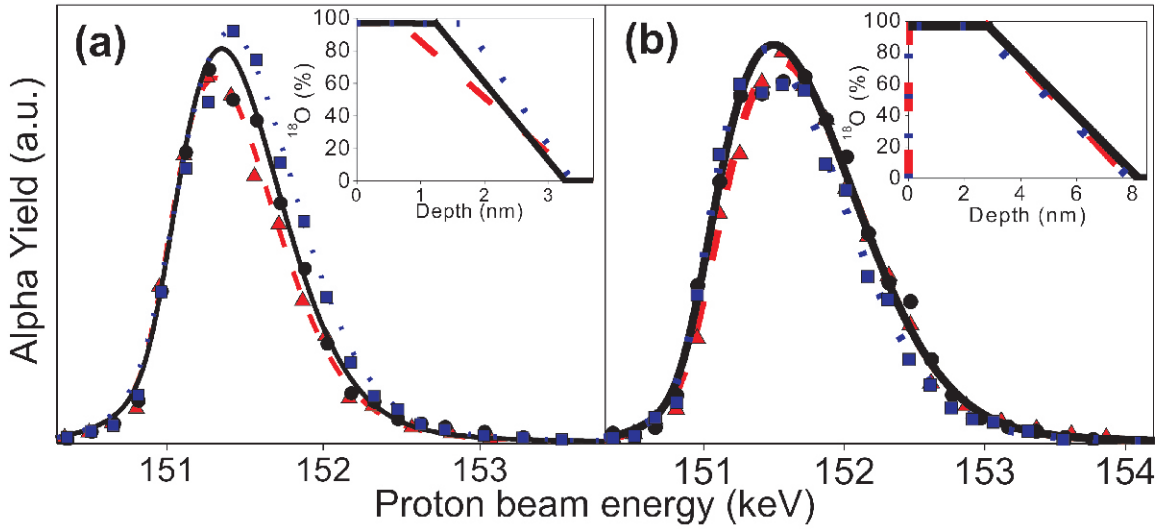

Figure 1. *Experimental (symbols) excitation curves of the $^{18}O(p,)^{15}N$ nuclear reaction around the resonance at 151 keV and the corresponding simulations (lines) for sample I (Δ and dashed line), II (° and solid line), and III (▪ and dotted line).* ***(a)*** *for the Si face and* ***(b)*** *for the C face samples.* ***Insets:*** *^{18}O profiles obtained from the simulation of excitation curves using the same line types. The horizontal line in the ^{18}O profile at 97% refers to the stoichiometric $Si^{18}O_2$ film, while the decrease on the ^{18}O concentration from this value to zero in the profile refers to the SiO_2/SiC interfacial region.*

Research outlook

As the SiO_2/4H-SiC interfacial thickness is related to electrical properties of SiC devices, the understanding of how the SiO_2/SiC interfacial region behaves when submitted to different sequential treatments has an important role in the fabrication of MOS devices based on SiC. Further investigations trying to relate these SiO_2/SiC interfacial region thicknesses of the present samples with D_{it} measurements are being performed.

Publications

[1] E. Pitthan, S. A. Corrêa, R. Palmieri, G. V. Soares, H. I. Boudinov, F. C. Stedile, *Effect of Reoxidations and Thermal Treatments with Hydrogen Peroxide in the SiO_2/SiC Interfacial Region*, Electrochem. Solid-State Lett., **14**, H368 (2011).

Photoluminescence of semiconductor nanostructures

P. Franzen

Introduction

We study the optimal deposition parameters to improve the photoluminescent emission from Si nanoparticles embedded in dielectric matrices, like Si_3N_4 and SiO_2. The samples are prepared by reactive sputtering of Si in Nitrogen or Oxygen environment and subsequently annealed in inert atmosphere to promote the aggregation of Si excess into nanoparticles. Size and concentration of nanoparticles are dependent on the relative amounts of N or O used during deposition, as well on the annealing temperature. Our samples typically show a complex emission band structure in the visible and/or near infrared. Some features of emission can be traced back to the sample peculiarities and thus provide a feedback to guide future sample processing.

Results

For the Si_3N_x matrix, we observed that optimal emission is reached with small amounts of Oxigen present in the deposition environment. Figure 1 (a) shows a typical emission spectra for both samples Si_3N_x samples have a fast decay time, < 1 µs. On the other hand, emission from samples with SiO_x matrices have much longer life times, in the range of µs. For those, we observed that the PL delay and emission maxima take place at the same wavelength. A sharp reduction in the decay time follows the band maximum in the lower energy direction. This behavior remains at lower temperatures, although the decay time increases exponentially.

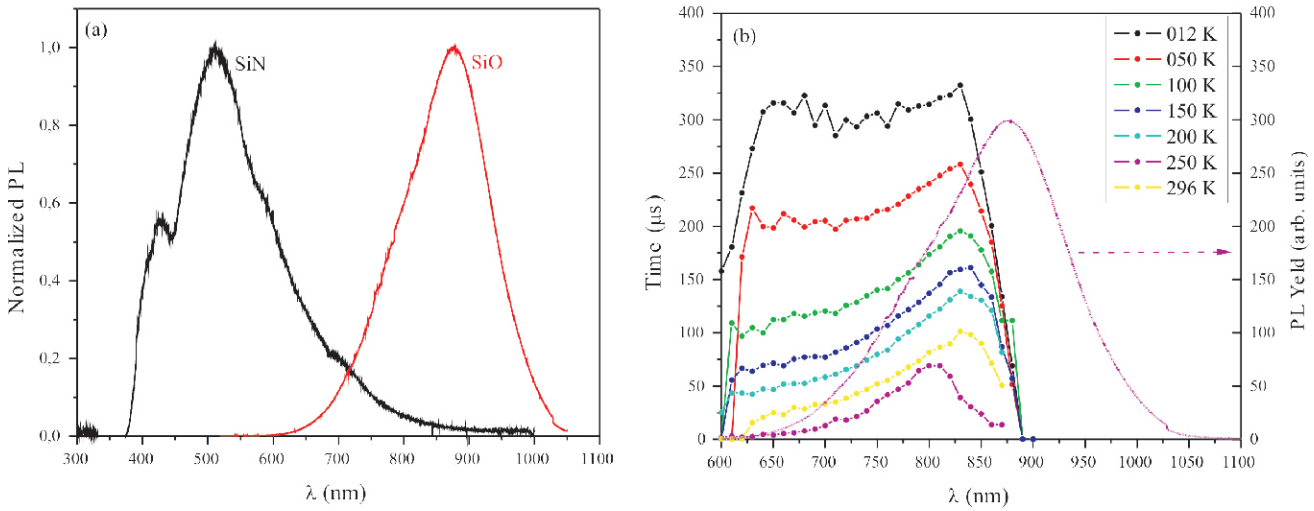

Figure 1 *(a) Photoluminescence spectra of Si_3N_x and SiO_x with embedded Si nanoparticles. (b) Delayed photoluminescence for different temperatures for a SiO_x sample. The instantaneous emission spectra at room temperature is added for comparison.*

Research outlook

The reactive sputtering technique will improve by further understanding the role of the many variables in the deposition and annealing processes and better understanding of the mechanisms of luminescent emission. In this sense, electroluminescence measurements could provide valuable additional information to picture the complex band structures in those materials.

Publications

[1] G. Sombrio, A.E.P. Mattos, P.L. Franzen, M.B. Pereira, H. Boudinov. *Photoluminescence in Non-Stoichiometric Silicon Nitride Films Obtained by Reactive Sputtering,* ECS Transactions, **39**, 315 (2011).

[2] A.E.P. Mattos, G. Sombrio, P.L. Franzen, M.B. Pereira, H. Boudinov. *Si Nanocrystals Embedded in SiO_2 Produced by Reactive Sputtering for Light Emission,* ECS Transactions, **39**, 103 (2011).

Nanoporous Aluminum Oxide Thin Films on a Si Substrate: Structural Changes as a Function of Interfacial Stress

Adriano F. Feil

Introduction

This work reports the effect of Al_2O_3-SiO_2 interfacial stress on porous anodic alumina (PAA) structures formed by anodizing 150 nm-thick-aluminum thin films (ATF) deposited on a silicon (Si) and glass substrate. The increase in the interfacial stress was achieved by growing thicker SiO_2 layers by anodizing the substrate after complete ATF-oxidation. Thicker SiO_2 layers induced structural changes on the PAA. The modifications of the PAA structure are related to the expansion of the SiO_2 layer, which exerts a bottom-up pressure on the PAA film to minimize the stress generated on the Al_2O_3-SiO_2 interface.

Results

Figure 1 represents a qualitative model of the structural change of alumina nanopores with increasing anodization time. The anodization process of a 150 nm Al thin film (Figure 1I) generates a layer of PAA with a heterogeneous distribution of D_P and D_{int} (Figure 1II). With the increase of anodization time, the ATF is entirely consumed, and the process of Si oxidation begins (Figure 1III). The formation of the SiO_2 layer leads to an expansion of the substrate layer under the PAA film due to differences in the density of the Si and SiO_2. This expansion generates a bottom-up force, increasing the interfacial stress between the Al_2O_3-substrate (black arrows in Figure 1III-VII).

Increasing the anodization periods leads to the formation of thicker SiO_2 layers, and a higher degree of interfacial stress will affect the PAA thin film (Figure 1III-VII). To minimize the energy of the system and prevent the collapse of the PAA film, there is likely a horizontal movement of the PAA walls (red arrows). This horizontal reaction force may lead to the shrinkage of small nanopores, explaining the decrease in the nanopore density and the increase in the D_P and D_{int}.

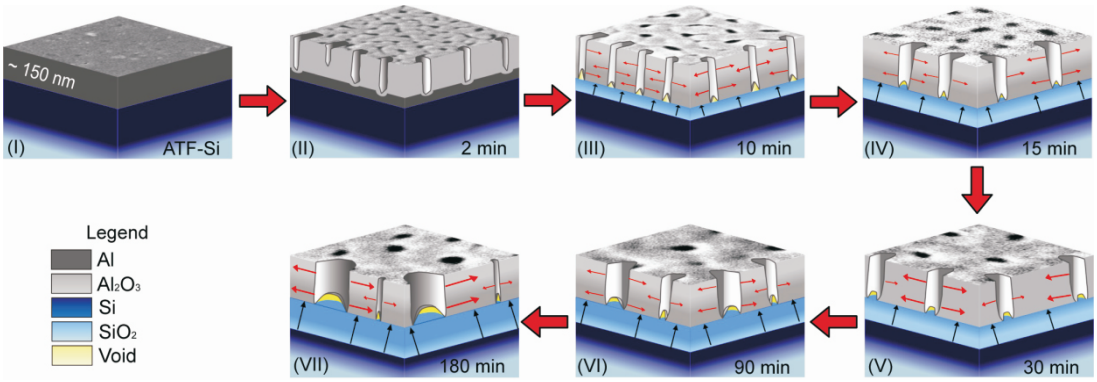

Figure 1 *Qualitative model of the structural change of alumina nanoporous structures, where the sequence of images represents the increase of the SiO_2 expansion layer as a function of anodization time. The 3D model was developed from the original SEM of the surface of the PAA images at each corresponding stage of anodization time.*

Research outlook

In summary, was demonstrated that the effect of Al_2O_3-SiO_2 interfacial stress on the PAA formed from 150 nm-thick-Al thin films deposited on a silicon substrate is related to the SiO_2 expansion. These findings can be used to design new ATF devices, thus making available a variety of technological applications for nanostructured-alumina thin films on Si substrates.

Publications

[1] A. F. Feil, P. Migowski, J. Dupont, L. Amaral, S. R. Teixeira, *Nanoporous Aluminum Oxide Thin Films on Si Substrate: Structural Changes as a Function of Interfacial Stress*, Journal of Physical Chemistry C, **115**, 7621-7627 (2011).

Distinguishing bulk traps and interface states in deep-level transient spectroscopy

A. Coelho

Introduction

Deep-level transient spectroscopy (DLTS) is a powerful electrical technique for characterizing discrete deep levels in semiconductors. In this work, we present a new method to distinguish discrete bulk deep level and interface states related peaks in DLTS spectra which is not destructive and can also be used for bulk traps with strong emission rate dependence on the electric field.

Results

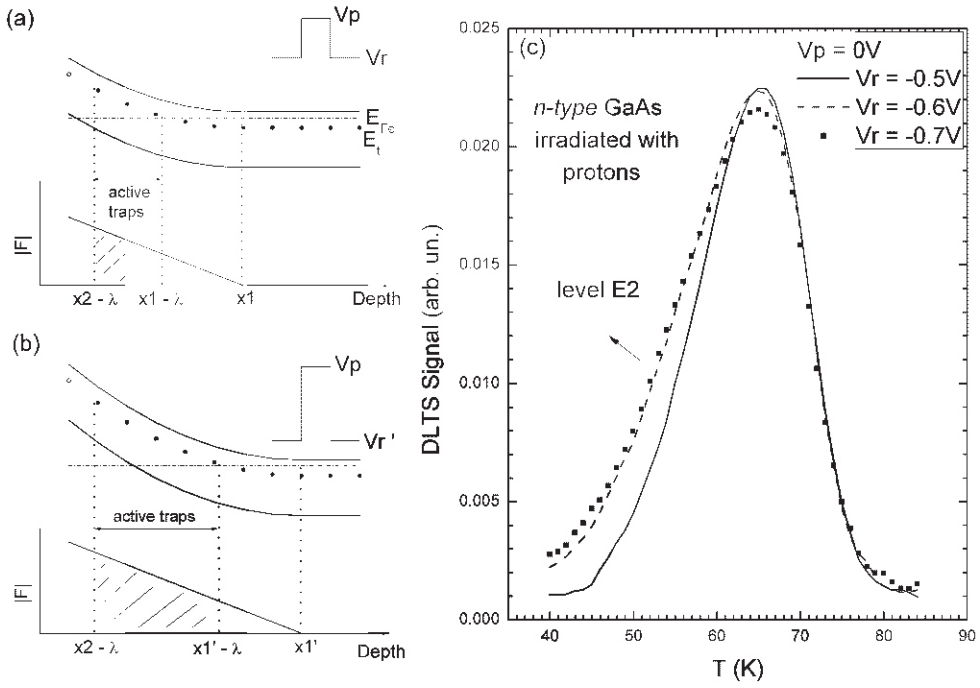

Figure 1 *Changes in a bulk deep level related DLTS peak due to a variation in reverse voltage. (a) Illustrates the active traps and the corresponding electric field region for a reverse voltage Vr, while (b) presents the active traps and electric field for the case of a reverse voltage Vr´ (increased pulse height). In (c), measured spectra for level E2 (a bulk trap level introduced by proton implantation in n-type GaAs which has a previously characerized strong emission rate dependence on the electric field) exemplify peak maximum shift and shape change for different reverse voltage values.*

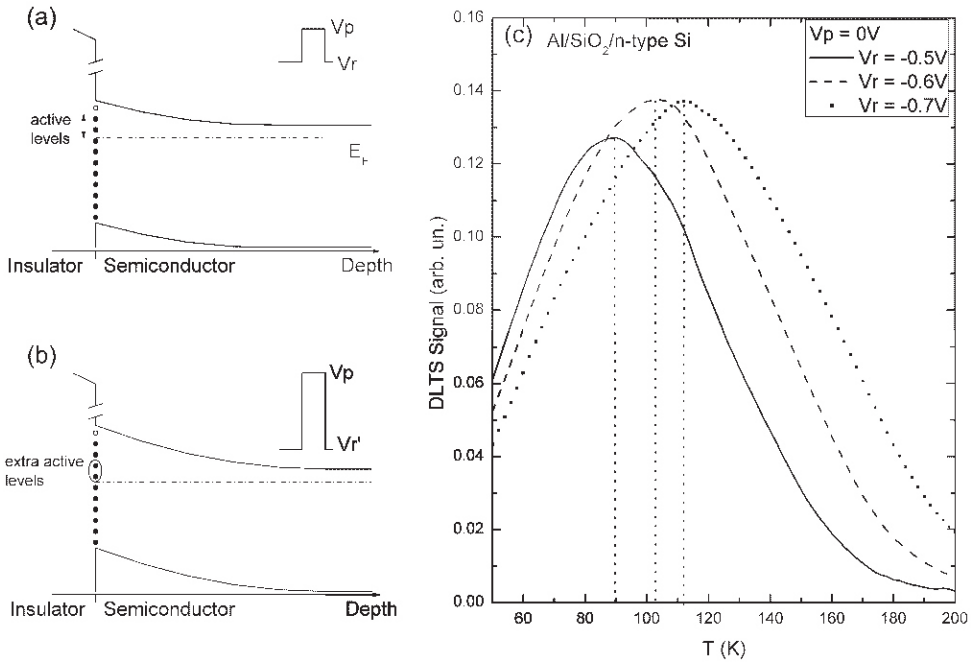

Figure 2 *Changes in a interface states related DLTS peak due to a variation in reverse voltage. (a) illustrates the active traps for a reverse voltage Vr, while (b) presents the active traps for the case of a reverse voltage Vr´ (increasing pulse height). In (c), measured spectra for a Al / thermal SiO_2 / n-type Si MOS capacitor exemplify peak maximum shift and shape change for varying Vr.*

Research outlook

A new method for the distinction of discrete bulk deep levels and interface states related peaks in deep-level transient spectroscopy spectra is proposed. The measurement of two spectra using different reverse voltages while keeping pulse voltage fixed causes different peak maximum shifts in each case: for a reverse voltage modulus increase, a bulk deep level related peak maximum will remain unchanged or shift towards lower temperatures while only interface states related peak maximum will be able to shift towards higher temperatures. This method has the advantages of being non-destructive and also works in the case of bulk traps with strong emission rate dependence on the electric field.

Publications

[1] A. V. P. Coelho, M.C. Adam, H. Boudinov , *Distinguishing bulk traps and interface states in deep-level transient spectroscopy, J. Phys. D: Appl. Phys.*, **44**, 305303 (2011).

GeSi nanoparticles in silica matrix studied by combined synchrotron radiation techniques

G. Azevedo

Introduction

The formation of GeSi nanoparticles (NPs) in SiO_2 matrix is studied here by synchrotron-based techniques. Shape, average diameter and size dispersion were obtained from grazing incidence small angle x-ray scattering. X-ray diffraction measurements were used to obtain crystallite sizes and composition via resonant (anomalous) measurements. By using these techniques as input for extended x-ray absorption fine structure analysis, the local composition surrounding Ge atoms is investigated. Although results for each of the methods above are commonly analyzed separately, the combination of such techniques leads to an improved understanding of nanoparticle structural and chemical properties.

Results

Samples we prepared by co-sputtering of SiO_2 anf Ge, followed by thermal annealing. The formation of spherical , compound GeSi (NPs) was checked by TEM and anomalous diffraction (a-XRD). Size distributions were determined by GISAXS. Information from TEM, a-XRD and GISAXS (figure 1) was utilized as input for the analysis of Ge-K Edge EXAFS spectra, which yielded the amorphous fraction and NP composition (figure 2).

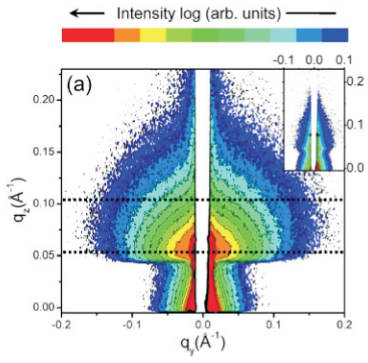

Figure 1 (a) *Two-dimensional GISAXS scattering pattern captured in the q_y-q_z plane by an image plate for the Ge nanoparticle sample (annealed for 2 hours). The inset shows the GISAXS result for an as-deposited Ge doped sample.*

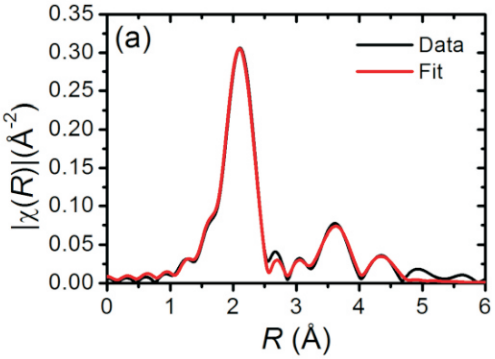

Figure 2 *Fourier Transfor of the k-weighted EXAFS signal (χ) (black line) and best fit (red line) obtained with input from a-XRD and GISAXS data, and the model described in Ref. [1]*

Conclusions

In this work, we have employed GISAXS, resonant and non-resonant XRD and EXAFS on the study of the composition, morphology and structure of GeSi nanoparticles. Besides direct measurements, we have obtained important indirect results only accessible by combining the results of the various techniques. By combining EXAFS and GISAXS, we determined the Ge concentration in the matrix; nanoparticle composition was obtained by EXAFS and anomalous XRD; comparing XRD and EXAFS, we determined the presence of compressive strain in the NPs. Finally, the fraction of Ge atoms located in amorphous and crystalline environments. The morphological properties of the nanoparticles were considered, including an estimation of the population of multi-domain NPs from the combined results from XRD, GISAXS and EXAFS.

Publications

[1] A. Gasperini, A. Malachias, G. Fabbris, G. Kellermann, A. Gobbi, E. Avendaño, G. Azevedo, *Investigation of indirect structural and chemical parameters of GeSi nanoparticles in silica matrix by combined synchrotron radiation techniques*, Journal of Applied Crystallography, **in press** (2011).

Passivation of electrical defects in SiO_2/4H-SiC structures

R. Palmieri

Introduction

In this work, SiO_2 was thermally grow on n- and p-type 4H-SiC using O_2 flux bubbled on hot hydrogen peroxide (H_2O_2), which is a strong oxidizing agent, and acts in silicon cabide (SiC) surface converting SiC_xO_y in SiO_2. Resulting structures were electrically characterized, and differences in D_{it} among n- and p-type 4H-SiC substrates were observed. To verify the H_2O_2 effects on SiC surface composition, oxidations of SiC using ^{18}O as a marker were performed, followed by thermal treatment with H_2O_2. Samples underwent probing by NRA and XPS. Results shown a reduction in silicon oxycarbides induced by H_2O_2. Electrical and physico-chemical data were related in order to explain differences among n- and p-type samples.

Results

Results shown the effects of using H_2O_2 as an oxidizing agent on the electrical and physico-chemical characteristics of the resulting SiO_2/4H-SiC structures. In comparison with similar structures prepared by 4H-SiC thermal oxidation using H_2O, reduced interface state densities were observed in n-type, while increased D_{it} in p-type counterparts. This effect was correlated with the decrease in SiC_xO_y compounds at the SiO_2/4H-SiC interface region as confirmed by two independent methods.

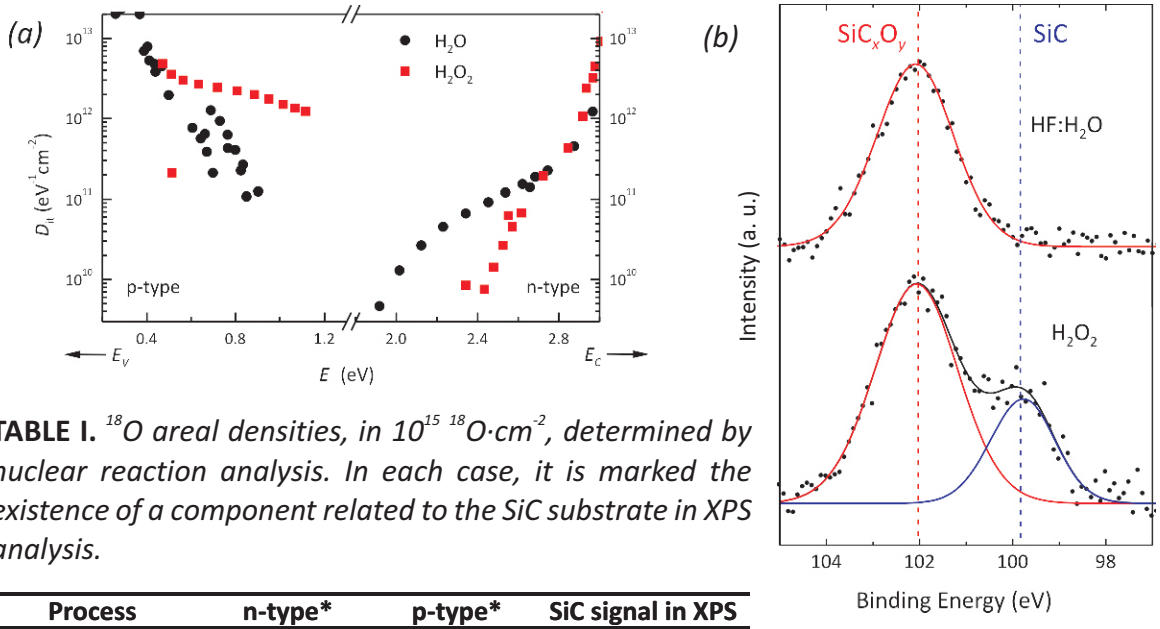

TABLE I. *^{18}O areal densities, in 10^{15} $^{18}O \cdot cm^{-2}$, determined by nuclear reaction analysis. In each case, it is marked the existence of a component related to the SiC substrate in XPS analysis.*

Process	n-type*	p-type*	SiC signal in XPS
$^{18}O_2$ oxidation	37.6	33.8	No
HF:H_2O	1.0	1.0	No
H_2O_2	0.4	0.3	Yes

Figure 1 *(a) Interface state density, D_{it}, as a function of energy for 4H-SiC MOS structures. Energy scale corresponds to the region of bandgap near the bottom of the 4H-SiC conduction band for n-type and near 4H-SiC valence band for p-type. Measurements were carried out between 30 and 300°C. (b) Si 2p regions of XPS spectra corresponding to p-types samples cleaned with HF:H_2O solution and H_2O_2 treatment. Points represent experimental data. Solid curves correspond to fitting components and their sum.*

Research outlook

Silicon carbide is a wide bandgap semiconductor with advantageous properties for high-power devices designed to work under extreme conditions, where silicon technology fails. Our results show that the combination of H_2O_2 passivation method with other well-established treatments may further improve the quality of both the n- and p-type SiO_2/4H-SiC interface and further enable the use of SiC in Microelectronics industry.

Publications

[1] E. Pitthan, S. A. Corrêa, R. Palmieri, G. V. Soares, H. Boudinov, F. C. Stedile, *Effect of Reoxidations and Thermal Treatments with Hydrogen Peroxide in the SiO_2/SiC Interfacial Region*, Electrochemical and Solid-State Letters, **14** H368 (2011).

[2] R. Palmieri, C. Radtke, H. Boudinov, E.F. da Silva, *Effect of H_2O_2 in passivation of n- and p-type 4H-SiC surfaces*, Physica Status Solidi C (2011).

Energy loss of swift H_2^+ and H_3^+ molecules in gold: Vicinage effects

S. M. Shubeita

Introduction

It is well known that the electronic energy loss of molecular ion beams in matter clearly differs from the interaction of the individual components of the molecule. The vicinage effect is a direct manifestation of coherent effects arising from the interference pattern of the wake potentials generated into the medium by each constituent of the molecule. In this case, the stopping ratio (defined as the ratio between the stopping power of the molecule and the sum of the stopping powers of its constituents) deviates from unity. Vicinage effects are effective as long as the molecular constituents move in a correlated manner. This work presents experimental and theoretical results of vicinage effects due to the interaction of H_2^+ and H_3^+ molecules with thin gold foils. Comparison with previous works are made.

Results

High energy resolution backscattering experiments were carried out at energies ranging from 80 up to 200 keV/nucleon for the H_2^+ molecules and up to 140 keV/nucleon for the H_3^+ molecules. The results show small enhancements (about 5% and 15% for H_2^+ and H_3^+ molecules respectively) of the stopping ratios (Fig. 1a). The values obtained by the simulation code SEICS indicate small vicinage effects as well and are in satisfactory agreement with the experimental data. However, these results are in clear disagreement with those reported in the seminal work of Brandt, Ratkowski and Ritchie [Phys. Rev. Lett. 33, 1325 (1974)] (Fig 1b, for H_2^+ ions).

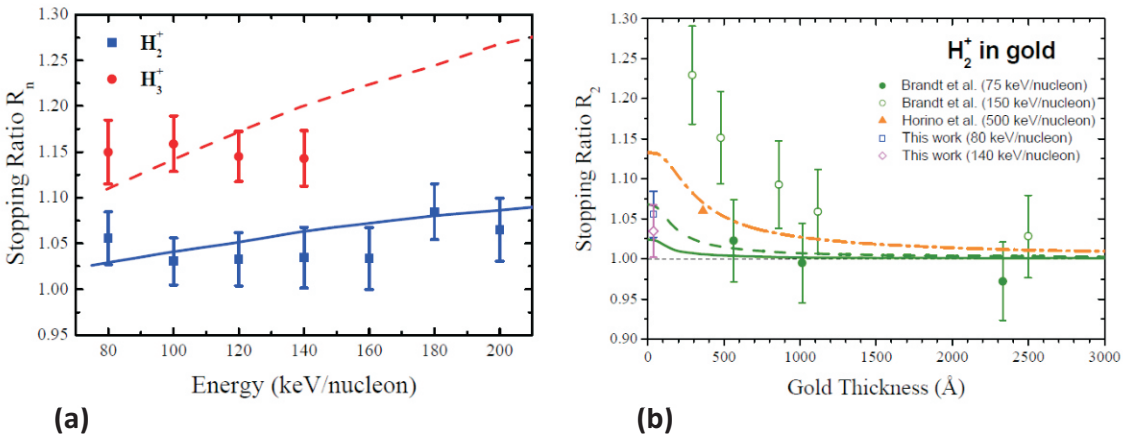

Figure 1 *(a) Experimental stopping ratios R_n for H_2^+ (n=2 for squares) and H_3^+ (n=3 for circles) molecules interacting with gold, as a function of the projectile energy. The target thickness is 37 Å. Full and dashed lines stand for the calculations of R_2 and R_3 based on the SEICS code respectively. (b) Stopping ratio for H_2^+ molecules as a function of the gold target thickness. Full and open circles: data from Brandt et al. at 75 and 150 keV/nucleon respectively; full triangle: data from Horino et al. at 500 keV/nucleon; open square: this work at 80 keV/nucleon; open diamond: this work at 140 keV/nucleon. Full, dashed and dash-dotted lines stand for the calculations based on the SEICS code at 75, 150 and 500 keV/nucleon respectively.*

Research outlook

A proper investigation of the experimental results concerning the stopping power of molecular ions relies on a realistic description of the energy-loss function of the material under study. Our results confirm a close correlation between the weight of the ELF at small transferred energies and the magnitude of the vicinage effects in the energy loss.

Publications

[1] S. M. Shubeita, P. L. Grande, J. F. Dias, R. Garcia-Molina, C. D. Denton, I. Abril, *Energy loss of swift H_2^+ and H_3^+ molecules in gold: Vicinage effects*, Phys. Rev. B, **83**, 245423 (2011).

Introducing electron capture into CasP*

P. L. Grande and G. Schiwietz

Introduction

Recent developments in the theoretical treatment of electronic energy losses of bare and screened ions in gases are presented. Specifically, the unitary-convolution-approximation (UCA) stopping-power model has proven its strengths for the determination of nonequilibrium effects for light as well as heavy projectiles at intermediate to high projectile velocities. The focus of this contribution will be on the UCA and its extension to specific projectile energies far below 100 keV/u, by considering electron-capture contributions at charge-equilibrium conditions.

Results

Figure 1 displays UCA results for the partial energy-loss cross sections related to excitation plus ionization of bound projectile electrons (purple dotted curve denoted by “loss”), excitation plus ionization of bound target electrons (blue dashed curve denoted by “target”), and electron transfer from bound target to bound projectile states (these charge-exchange processes are denoted by “capture” and are displayed as an olive-colored dashed-dotted curve The comparison shows good agreement between UCA and experimental data at intermediate to high energies. At low kinetic energies (below20 keV) the maximum deviation between experiment and UCA reaches 20% for the Ne and Kr targets. For the Ar target, however, we find good overall agreement between experiment and ab initio theory.

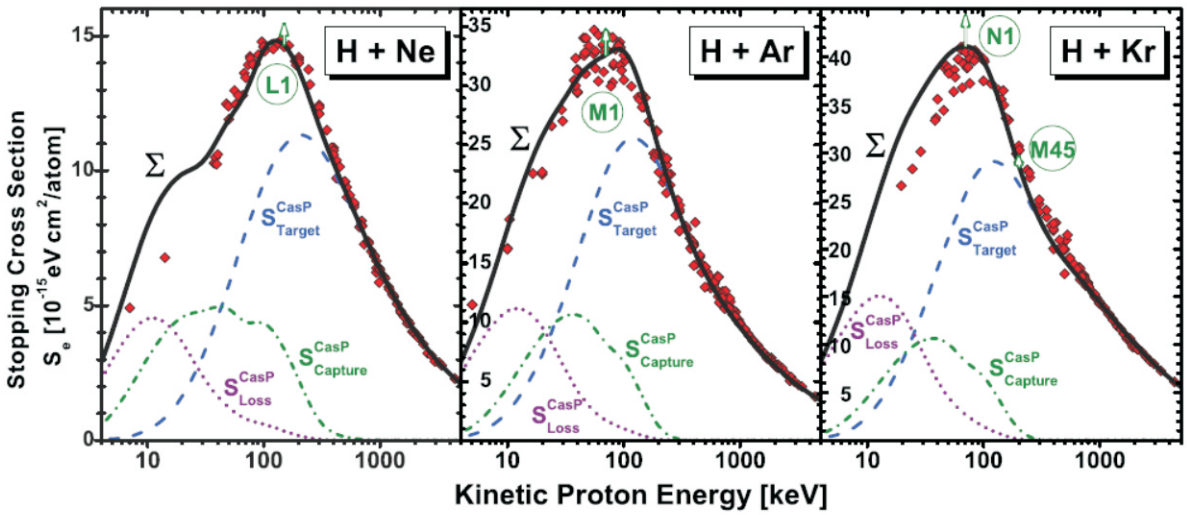

Figure 1 *Projectile-energy dependence of the electronic energy loss of charge-equilibrated hydrogen beams in different heavy rare gases (Ne, Ar, and Kr). Experimental values (red diamonds) are taken from the data collection of Paul . Dashed, dotted, and dashed-dotted curves are charge-weighted partial energy-loss cross sections. The solid black curve denoted corresponds to the sum of these partial contributions. The open arrows, shell indicators (L1,M1,N1,M45) and further details are explained in ref[1].*

Research outlook

We have successfully included the electron-capture contribution into the CASP energy-loss code. Good agreement with experimental data has been achieved for high to intermediate energies. At energies below ~20 keV, however, we find significant deviations between experiment and theory in some cases.

*www.casp-program.org

Publications

[1] G. Schiwietz and P.L. Grande, *Introducing electron capture into the unitary-convolution-approximation energy-loss theory at low velocities*, Physical Review A, **84**, 052703 (2011) .

Structural control of gold nanoparticles self-assemblies by layer-by-layer process

G. Machado, A. F. Feil, P. Migowski, L. Rossi, M. Giovanela, J. Crespo, L. Miotti, M. A. Sortica, P. L. Grande, M. B. Pereira, R. R. B. Correia

Introduction

This work presents a novel way to introduce gold nanoparticles (Au NPs) in a multilayer polymer produced by the layer-by-layer (LbL) assembling technique. The technique chosen shows that, depending on the pH used, different morphological structures can be obtained from monolayer or bilayer Au NPs. The MEIS and RBS techniques allowed for the modeling of the interface polymer- NPs, as well as the understanding of the interaction of LbL system, when adjusting the pH in weak polyelectrolytes. The process reveals that the optical properties of multilayer systems could be fine tuned by controlling the addition of metallic nanoparticles, which could also modify specific polarization responses.

Results

Figure 1 shows the sequence of 2D (energy/angle) MEIS spectra (a, b, c and d) and 1D, for a fixed scattering angle of 120 degrees, (e, f, g and h) of the four different LbL systems (samples S1, S2, S3 and S4 described in the text), (i, j, l and m) correspond to NPs configurations that best fit the MEIS results for the samples S1, S2, S3 and S4 respectively.

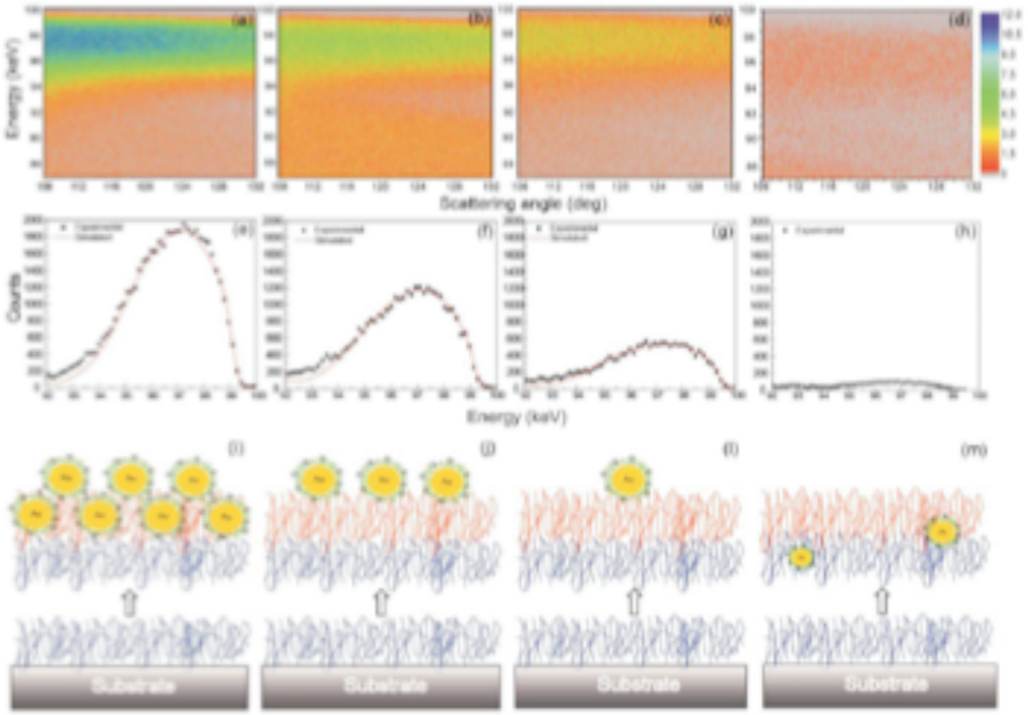

Research outlook

The dispersion of the NPs in the system LbL can change dramatically depending of pH value in both-colloidal gold solution and PEM films. For the PEM films (PAH7.5/PAA3.5)20 the variation of the Au NPs pH from 6.0 (S1) to 3.0 (S3) changed the amount of Au NPs on the polyelectrolyte multilayer, respectively forming a compact bilayer and a incomplete monolayer with Au NPs on the LbL surface. When PEM films (PAH3.5/PAA3.5)20 were immersed in colloidal gold solution at pH 3.0 (S2) a compact monolayer was observed while at pH 6.0 (S4), was verify a homogeneous dissemination of Au NPs through them.

Publications

[1] G. Machado, A. F. Fail, P. Migowski, L. Rossi, M. Giovanela, J. S. Crespo, L. Miotti, M. A. Sortica, P. L. Grande, M. B. Pereira, R. R. B. Correia, *Structural control of gold nanoparticles self-assemblies by layer-by-layer process*, Nanoscale **3**, p. 1717 (2011).

Effects of ion irradiation on embedded Ge nanoparticles

L. L. Araujo

Introduction

Ion beam tailoring of embedded nanoparticles (NPs) has been proposed as a means to improve their technologically relevant properties through controlled changes in NP size and shape. Many studies so far have concentrated on ion beam modification of metal NPs embedded in silica, but not much is known about the response of embedded semiconductor nanoparticles to ion irradiation.

In this study we followed the structural and morphological evolution of Ge NPs embedded in silica during ion irradiation at two distinct regimes: “low energy” irradiation with 5 MeV Si ions and “high energy” irradiation with 27, 54 and 185 MeV Au ions.

Results

Unlike observed for metal NPs, ion irradiation of embedded Ge NPs ultimately leads to their amorphisation. The fluence required to amorphise Ge NPs is much smaller than that required for bulk Ge, no matter if the amorphisation proceeds via nuclear stopping (atomic collisions - “low energy” regime) or via electronic stopping (thermal effects - “high energy” regime).

A change in Ge NP shape was also observed at the “high energy” irradiation regime, always at fluences higher than those required for amorphisation, suggesting the NPs only change shape after becoming amorphous. Elongation of Ge NPs both parallel and perpendicular to the beam direction was observed, depending on NP size and irradiation conditions. This is in contrast to the results for metal NPs, where elongation is always parallel to the beam.

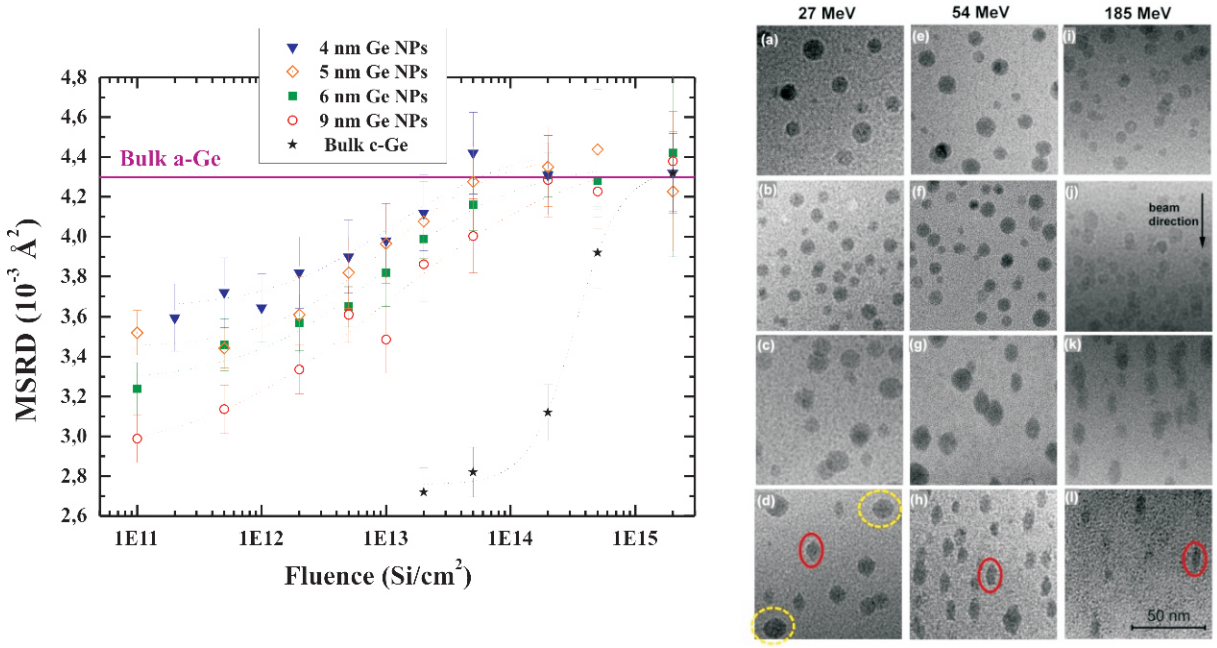

Figure 1 *(left) Mean squared radial displacements (MSRD) obtained from XAS measurements for Ge NP distributions with different mean sizes and bulk Ge, after irradiation with 5 MeV Si ions. The MSRD increases with irradiation fluence until reaching the value for amorphous Ge, which happens faster for smaller NPs. (right) TEM images for Ge NP samples irradiated with 27 (left), 54 (centre) and 185 (right) Mev Au ions. For the lowest energy elongation both parallel (highlighted in red) and perpendicular (highlighted in yellow) to the ion beam is observed, whereas only elongation parallel to the beam direction is observed for the other irradiation energies.*

Research outlook

Further studies on other embedded semiconductor NP systems (such as GaAs and Si NPs in silica) are needed to verify if our observations can be extended to semiconductor NPs in general or if they are peculiar to the Ge NPs case.

Publications

[1] L. L. Araujo, R. Giulian, D. J. Sprouster, M. C. Ridgway, et al, *Structural properties of embedded Ge nanoparticles modified by swift heavy ion irradiation*, Physical Review B (submitted) 2011.

Fracton to Phonon Transitions

C. R. Da Cunha

Introduction

Materials with fractal geometry typically have localized vibrations whose quantization is referred to as a fracton. The presence of fractons in a material can cause anomalous diffusion with square mean displacement obeying a power law related to its fractal dimension which reduces the thermal conductivity. Here, we use the atomistic Green's function formalism to study the transition from fracton to phonon states in a Sierpinski triangle lattice submitted to different levels of structural disorder. The transmission function, local density of states and correlation properties are studied.

Results

Figure 1a shows correlation dimension curves for a Sierpinski triangle. It indicates that for small levels of disorder, as the self-similarity level increases, the correlation dimension of the density of states tends to peak at a value near the unity, indicating a transition in topology from a fractal to an Euclidean space. Figure 1b shows the average cluster size indicating that although we are introducing disorder in the system, there may be a better coupling between points in the fractal as the fractonic states are broken and percolating clusters are formed – a behavior similar to the small-world effect.

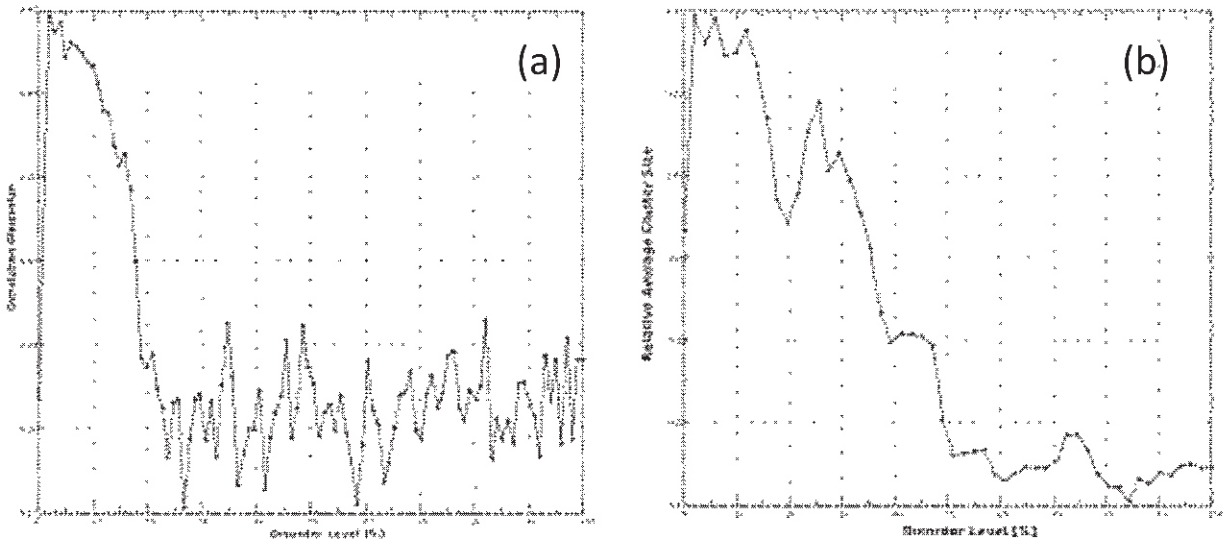

Figure 1 *(a) The correlation dimension as a function of the structural disorder level for a Sierpinski lattice with self-similarity level of seven. (b) The relative average cluster size for the same lattice as a function of the level of structural disorder.*

Research outlook

The tuning localization found in this theoretical toy model is a result somewhat different from what Anderson localization predicts for regular geometries. This has to be further explored in more sophisticated models. Moreover, aerogels will be used as an experimental lab to test these ideas.

Publications

[1] E. L. Da Rocha, C. R. Da Cunha, *The transition from fracton to phonon states in a Sierpinski triangle lattice*, Chaos, Solitons & Fractals, **44**, 241 (2011) .

Influence of light-ion irradiation on the heavy-ion track etching of polycarbonate

R. M. Papaléo

Introduction

The damaged region created around swift heavy-ion trajectories in dielectric materials often exhibits a different chemical reactivity than the unmodified surroundings. Therefore, when the bombarded region is exposed to an appropriate etching agent, the ion tracks can be developed to tailor micro- or nanostructures on surfaces or to modify materials properties. Because of its excellent mechanical properties and high sensitivity to the track etching, polycarbonate (PC) has been extensively investigated, and is commercially available as precise pore diameter membranes for filtering, detection of contaminants, and other biomedical applications. In this work, we investigated the effect of a 2 MeV H^+ treatment on the etching response of the foils to 18 MeV Au^{7+} ions.

Results

Below, the pore diameter dependence with H^+ fluence f is shown (Fig. 1). The proton irradiation causes initially a decrease in the mean etched pore size, as compared to samples only bombarded by Au ions, reaching a minimum at H^+ fluences around 2-5 x10^{13} cm^{-2}, whilst at higher f the pore size starts to grow again.

This effect is attributed to the action of two competitive processes that dominate in different fluence regimes. The decrease in the pore radii at low fluences is attributed to an increase in crystallinity induced by the proton beam. As the total dose builds up, this effect is surpassed by chain scission and amorphisation that grow at a lower rate and cause the pore radii to increase again.

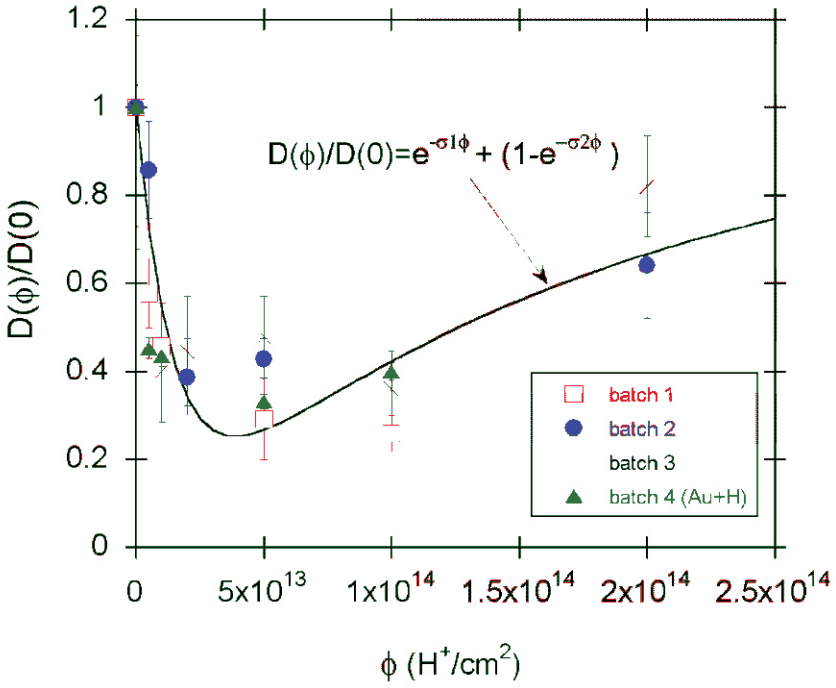

Figure 1 *Normalized diameter of the etched pores (D(f)/D(0)) as a function of H^+ fluence f, for four batches of samples. D(0) is the diameter in the samples bombarded with Au only. The solid line is the best fit of the function to the data points, obtained with $s_1=7.2\times10^{-14}$ cm^2 and $s_2=5.7\times10^{-15}$ cm^2.*

Publications

[1] Thomaz, R. S.; Souza, C. T.; Papaléo, R. M. *Influence of light-ion irradiation on the heavy-ion track etching of polycarbonate. APPL PHYS A-MATER*, **v. 104**, p. 1223-1227 (2011).

Shape transformation of embedded metal NPs by swift heavy ion irradiation

R. Giulian

Introduction

Elemental metal nanoparticles (NPs) embedded in a-SiO_2 and subjected to swift heavy ion irradiation (SHII) can undergo an intriguing shape transformation where once-spherical NPs become progressively more rodlike with the direction of elongation aligned along that of the incident ion. Freestanding metallic NPs irradiated under comparable conditions do not change shape, demonstrating the embedding a-SiO_2 matrix must have a role in the shape transformation process. For this report, we examine the SHII-induced elongation of ten embedded, elemental metal NP systems using a common irradiation condition to enable the identification of subtle, metal-specific differences and demonstrate that the thermodynamic properties of both the matrix and metal are intrinsic to the shape transformation process.

Results

Spherical NPs below a threshold diameter did not elongate while those of greater size progressively transformed to a rodlike shape of fixed width independent of length. Utilizing a common irradiation condition enabled us to identify metal-specific differences in both the spherical NP threshold diameter and elongated NP width and relate such differences to the width of the molten ion track in a-SiO_2 and the energy density per atom required for vaporization of the metal NP.

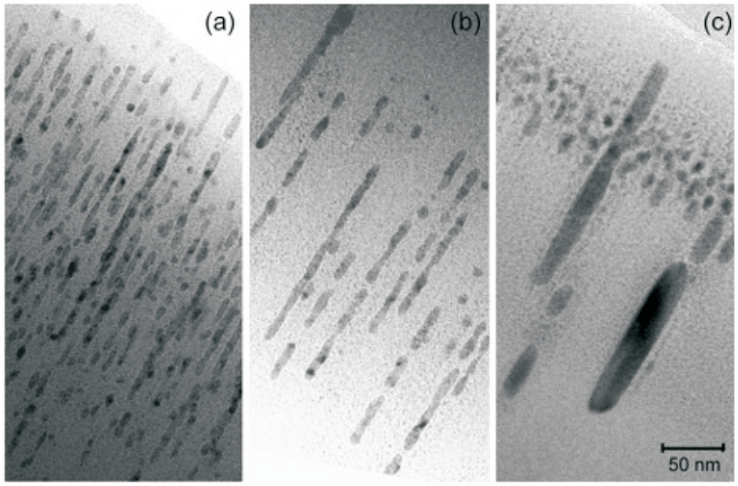

Figure 1 XTEM images of (a) Ni, (b) Cu and (c) Bi NPs following SHII. The incident-ion direction was from the top right to bottom left of the image.

Research outlook

This work will be extended to the study of ferromagnetic NPs embedded in antiferromagnetic matrices, aiming at tracking magnetic properties by changing the NP shape and structure with SHII.

Publications

[1] M.C. Ridgway, R. Giulian, D.J. Sprouster, P. Kluth, L.L. Araujo, D.J. Llewellyn, A.P. Byrne, F. Kremer, P.F.P. Fichtner, G. Rizza, H. Amekura, M. Toulemonde, *Role of thermodynamics in the shape transformation of embedded metal nanoparticles induced by swift heavy ion irradiation*, Physical Review Letters, **106**, 095505 (2011).

Interaction of Aluminum Oxide with Germanium during Thermal Annealing in Ar, N_2/H_2, O_2, or H_2O

C. Radtke

Introduction

Aluminum oxide (Al_2O_3) is an interesting alternative for Ge passivation. First-principle investigations demonstrated that Al incorporation close to dielectric/Ge interface tends to form germanate layers, resulting in a surface-state free Ge energy band gap. Incorporation of impurities like C and hydroxyl groups in Al_2O_3 may have a decisive role in the interaction of the deposited material with the substrate. To clarify this point, a physico-chemical description of the Al_2O_3/Ge interface is needed, especially concerning the modifications induced by different thermal treatments and the incorporation of oxidizing species in the dielectric layer.

Results

Al_2O_3 films were deposited on Ge substrates by reactive sputtering and submitted to post-deposition annealings (PDAs) in argon, forming gas, oxygen, or water vapor at 350 or 500°C for 30 min. Photoelectron spectroscopy evidenced that Ge was oxidized during the deposition process. Thermal annealing in argon or forming gas reduced the amount of oxidized Ge. Oxygen and water strongly interacted with the Ge substrate. Particularly for water at 500°C, ion scattering analyses evidenced the presence of Ge throughout the Al_2O_3 layer and on the sample surface. This was attributed to the formation and desorption of GeO from the dielectric/Ge interface.

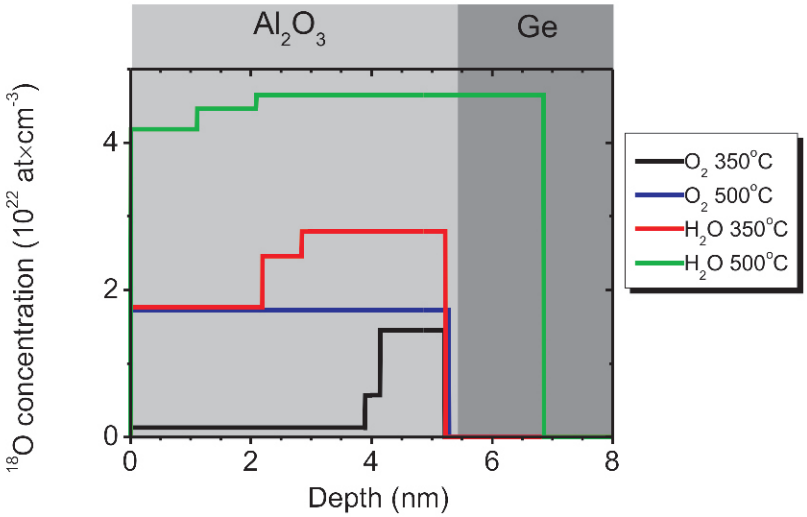

Figure 1 ^{18}O concentration profiles obtained by NRP of Al_2O_3/Ge samples annealed in the conditions listed in the caption. Behind the profiles, there is a sketch indicating the dielectric/semiconductor interface position of the as deposited sample as determined by TEM.

Research outlook

These results have strong technological implications, considering the importance of deposition processes in microelectronic industry (which uses water vapor as a precursor) and the processing temperatures used in device fabrication.

Publications

[1] C. Radtke, N.M. Bom, G.V. Soares, C. Krug, and I.J.R. Baumvol, *Interaction of Aluminum Oxide with Germanium during Thermal Annealing in Ar, N_2/H_2, O_2, or H_2O*, ECS Transactions, **41**, 21 (2011).

V_2O_3 (0001) Surface Termination: Phase Equilibrium

A. Hentz

Introduction

Oxide surfaces, and particularly those of vanadium oxides, play a major role in heterogeneous catalysis, yet there have been very few quantitative experimental structure determinations. The (0001) faces of the corundum-phase structure V_2O_3 is particularly interesting because there are several distinctly different atomic layers at which the bulk structure might be terminated. Three distinct stoichiometric terminations of this bulk structure can be envisaged, namely, oxygen … VVO_3, full-metal … O_3VV, and half-metal … $V'O_3V$.

The studies reported here used the techniques of medium-energy ion scattering (MEIS) and low-energy noble gas impact-collision ion scattering spectroscopy with detection of neutrals (NICISS) using, respectively, 100 keV H^+ and 3 keV He^+ incident ions in order to study the upper-most layers of this system.

Results

Figure 1-a shows experimental MEIS blocking curves of scattering from V atoms, recorded at two different crystallographic incidence directions, compared with the results of simulations using the VEGAS computer code. Figure 1-b shows the key results of the NICISS experiments; azimuthal scans of the scattered ion yield from V atoms, recorded at two different grazing incidence angles, are compared with the results of simulations using the FAN computer code. For all these data, the simulations based on the reconstructed O_3 termination model provide a greatly superior description of the experimental data.

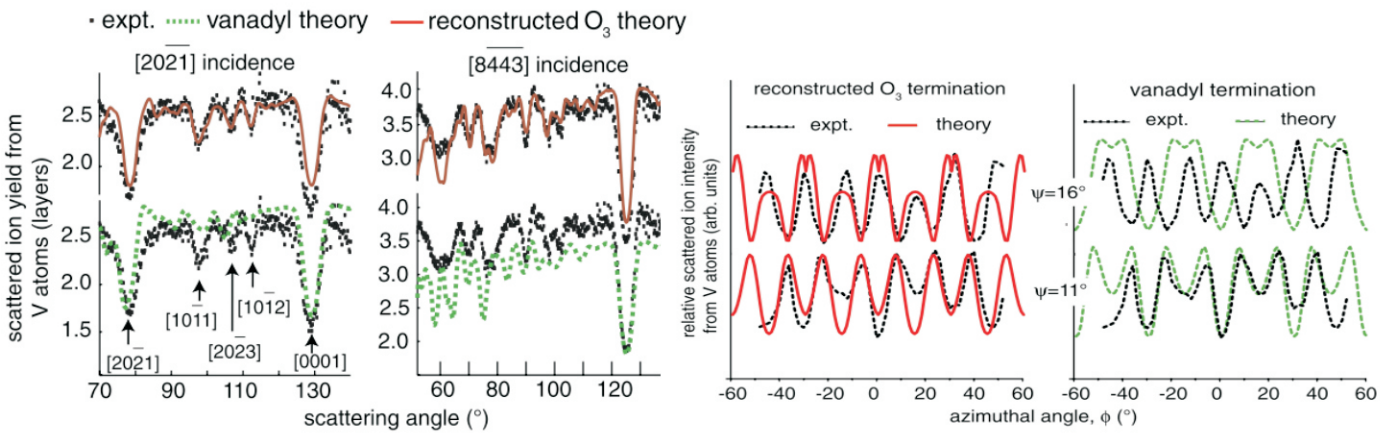

Figure 1 *(a) Comparison of experimental 100 keV H^+ MEIS blocking curves from V_2O_3 grown on Au(111), recorded in two different incidence directions, with the results of VEGAS simulations for the reconstructed O_3 and vanadyl termination models. The scattered ion yield is expressed in terms of the number of contributing atomic layers. (b) Comparison of experimental 3 keV He^+ NICISS azimuthal scans from V_2O_3 (0001) grown on Cu_3Au (100), recorded at two different grazing incidence angles, with the results of simulations for the reconstructed O_3, and the vanadyl termination models.*

Research outlook

Ion beam techiques, namely medium energy ion scattering (MEIS) and gas impact-collision ion scattering spectroscopy with detection of neutrals (NICISS), are used under shadowing conditions in order to improve surface sensitivity, allowing for a better understand of the atomic structure of the top-most layers of crystalline materials. In this particular work, we analysed the V_2O_3 termination when grown on top of metallic substrates.

Publications

[1] A. J. Window, A. Hentz, A., et al., *V_2O_3 (0001) Surface Termination: Phase Equilibrium*, Physical Rewiew Letters, **107** 016105 (2011).

Structural and photoluminescence properties of Si nanoclusters obtained by ion implantation into Si_3N_4 films

U. S. Sias

Introduction

We report structural and photoluminescence (PL) results obtained by Si implantation into stoichiometric Si_3N_4 nitride films. The Si excess was obtained by a 170 keV Si, with Ö = 1 x 10^{17} Si/cm^2. The annealing temperature was varied between 350 and 900 °C. PL measurements were done using a 488 nm Ar laser as an excitation source and two superimposed broad PL bands were obtained. The maximum PL yield was achieved when the samples were annealed at 475 °C. TEM measurements show the formation of nanoclusters distributed almost uniformly along the film. The characteristics of the PL bands did not change despite changes in the implantation and annealing parameters.

Results

Samples were implanted at RT and annealed for one hour in a N_2 atmosphere in a range of temperatures between 350 and 900 °C.
In Fig. 1a several PL spectra from samples annealed at different temperatures are shown. As can be observed, all PL spectra are broad, with two superimposed bands centered at around 760 and 900 nm, with position and shape independent of the annealing temperature. In Fig. 1b the results of the present experiment are summarized, showing that the maximum PL yield was obtained with the 475 °C annealing temperature. In Fig. 1c is displayed a TEM micrograph of a sample annealed at 475 °C for 1 h. As can be observed, the a-Si NCs can be found almost through the whole film with a slight higher density at the implanted region. In Fig. 1d are presented the corresponding histograms of samples annealed at 350, 475 and 600 ºC for 1 h.

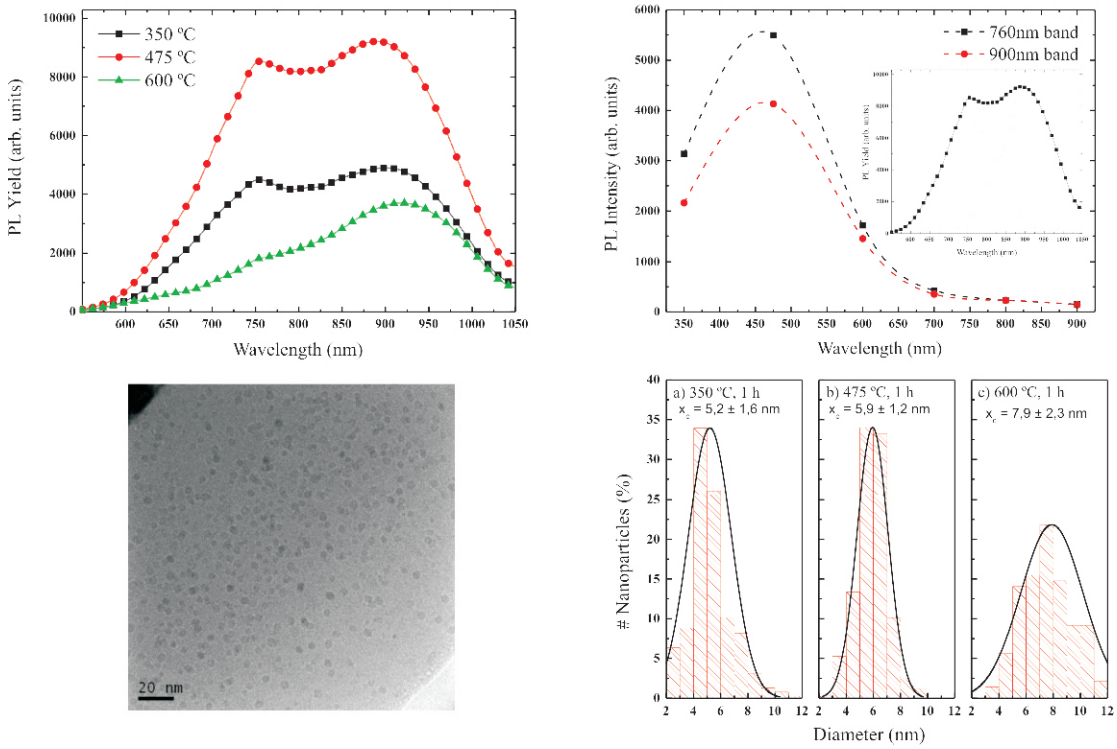

Figure 1 *(a) PL spectra of samples implanted at RT and annealed at different temperatures in N_2, for 1h. (b) Summary of the present experiment. Inset: Gaussian-fit of the two superimposed PL emission bands. (c) TEM image of a sample implanted at RT and annealed at 475 °C. (d) Histograms of samples implanted at RT and annealed at different temperatures.*

Research outlook

The present results are in qualitative agreement with those reported by [2] which used non-stoichiometric films produced by the PLCVD technique. A major finding of the present work is that the maximum PL emission yield was found with a much lower annealing temperature (475 °C) than the one used in Ref. [2] (700 °C). As the shape and position of the PL bands did not change with the mean nanoparticle size, it confirms that this bands have they origin in radiative interface states as proposed by [2].

Publications

[1] F.L. Bregolin, M. Behar, U.S. Sias, E.C. Moreira, J. Lum., **131**, 2377 (2011).
[2] L. Dal Negro et al., Appl. Phys. Lett. 88, 233109 (2006).

TiO_2 nanotubes decorated with Au nanoparticles for H_2 production

Guilherme J Machado, Adriano Feil, and Lívio Amaral

Introduction

The search for alternative and renewable energy has intensified in recent years. Hydrogen is a great alternative, but its production is still a problem, since 95% of hydrogen today is produced from natural gas and only 5% is produced through renewable sources. The production of hydrogen by splitting of water using TiO_2 nanotubes (TiO_2 NTs) as semiconductor and solar radiation becomes attractive, but the efficiency of this process is low. There are three factors leading to low efficiency of TiO_2, i) Recombination of photo-generated electron/hole pairs, ii) fast backward reaction and iii) inability to utilize visible light. Noble metals, have been reported to be very effective for enhancement of TiO_2 photocatalysis [1].

Results

This paper aims to show a way to decorate the TiO_2 NTs surface with Au nanoparticles. The TiO_2 nanotubes were produced by anodization in a electrolyte of ETG +10 wt% H_2O +0.25 wt% NH_4F to 20V for 2h [2]. Once the nanotubes were annealed in air at 400 ° C for 3h. Au NPs on the TiO_2 nanotubes surface were formed by two methods: i) sputtering and ii) ion implantation. The hydrogen production was carried in a photocatalytic reactor exposed to a 400W Xe-Hg lamp. 1.9 M glycerin was used for photolysis medium. The quantification of hydrogen production were performed by gas chromatography.

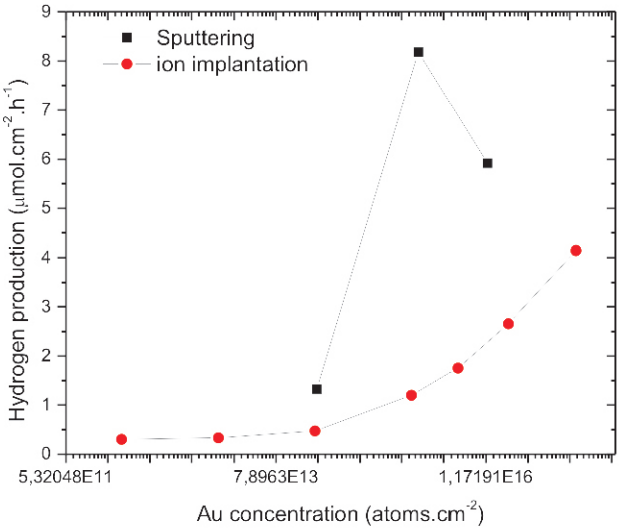

Figure 1. Hydrogen production rate as a function of Au concentration on TiO_2 nanotubes surface.

Research outlook

TEM images show a higher concentration of nanoparticles for the samples subjected to sputerring. Possibly the difference in hydrogen production is related to the quantity and size of Au nanoparticles. XRD analysis show that the implanted samples, possibly Au ions are substituting Ti atoms, causing a different phenomenon than samples decorated with sputtering.To improve the interpretation of results is necessary to reproduce the samples and submit them to the analysis of XPS and UV-Vis.

Publications

[1] 1. M. Ni, M. K. H. Leung, D. Y. C. Leung and K. Sumathy, *Renewable & Sustainable Energy Reviews*, 2007, **11**, 401-425.

[2] A. F. Feil, P. Migowski, F. R. Scheffer, M. D. Pierozan, R. R. Corsetti, M. Rodrigues, R. P. Pezzi, G. Machado, L. Amaral, S. R. Teixeira, D. E. Weibel and J. Dupont, *J. Braz. Chem. Soc.*, 2010, **21**, 1359-1365.

Intermixing between HfO_2 and GeO_2 films deposited on Si(001) and Ge(001):Role of the substrate

G.V. Soares

Introduction

There is a current research effort on high-mobility semiconductors due to their potential applications in high performance metal-oxide-semiconductor field effect transistors. Germanium (Ge) is a particularly relevant candidate for next generation devices, but the necessary surface passivation, is still under investigation. Use of a high-k dielectric has been demonstrated to some extent and HfO_2, now incorporated to advanced Si technology, is one of the most promising dielectrics for Ge.

Results

Figure 1 (left-hand side) shows a cross-sectional transmission electron microscopy (XTEM) image of the as-deposited sample on Ge. A well defined interface is observed between amorphous HfO_2 and GeO_2. However, Fig. 1(righ-hand side) presents Hf 4*f* photoelectron spectra for samples on Ge and Si, both as-deposited and annealed at 600°C for 1 h. Ge samples annealed at 600°C showed an additional spectral component assigned to Hf-O-Ge bonding. This result indicates that the substrate onto which the HfO_2/GeO_2 stacks are deposited plays a major role regarding thermal stability. The process that triggers chemical interaction between HfO_2 and GeO_2 on Ge above 500°C is absent on Si.

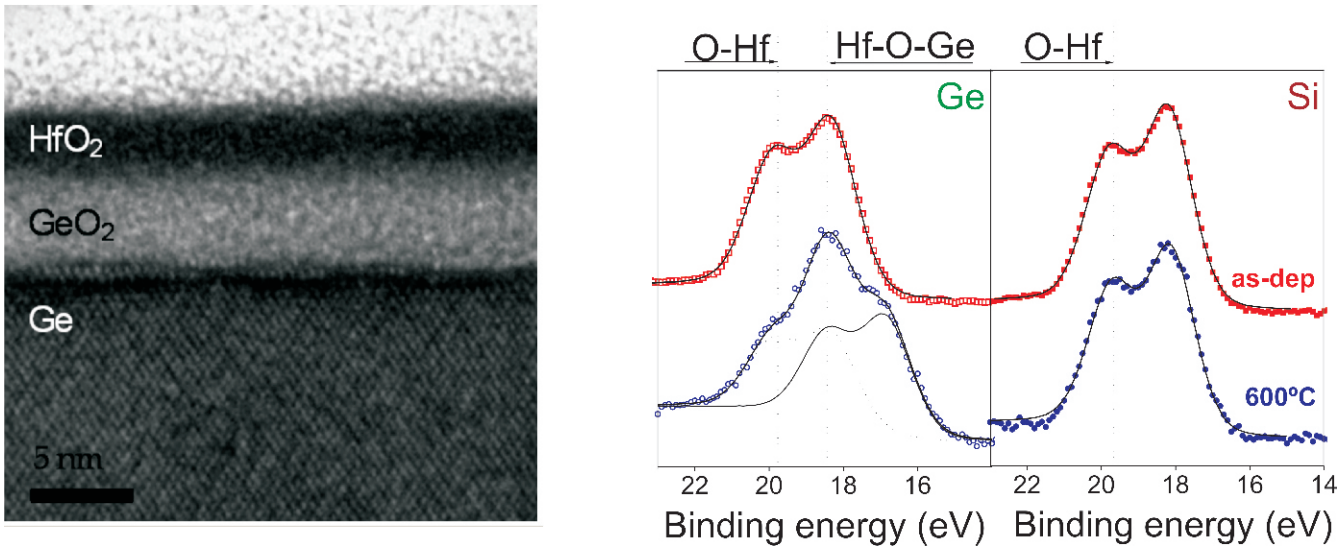

Figure 1 *Left-hand side: XTEM image of the HfO_2/GeO_2/Ge as-deposited sample. Right-hand side:Hf 4f XPS spectra of HfO2/GeO2 layers on Ge (open symbols) and on Si (full symbols) in samples as-deposited (red) and annealed at 600°C for 1 h (blue).*

Research outlook

Combined use of photoelectron spectroscopy and ion beam analysis revealed that the HfO_2/GeO_2 stack deposited on Si is stable at up to 600°C. Annealed samples on Ge yielded direct evidence of migration and loss of both Ge and O. This was understood as due to the formation of volatile GeO at the GeO_2/Ge interface. In addition, hafnium germanate formed at 600°C. Our data indicates that at 500°C and above HfO_2/GeO_2 stacks are stable only if isolated from the Ge substrate.

Publications

[1] G.V.Soares, C. Krug, L. Miotti, K.P. Bastos, G. Lucovsky, I.J.R. Baumvol, C. Radtke, *Intermixing between HfO2 and GeO2 films deposited on Ge(001) and Si(001): Role of the substrate*, Applied Physics Letters,**98**, 131912 (2011) .

FM/AF exchange coupling when $T_C << T_N$

K.D. Sossmeier

Introduction

In a magnetization hysteresis loop measurement, the exchange bias (EB) manifests itself as a shift of the loop to either the negative or positive direction of the magnetic field axis. This effect is usually observed in systems composed of a ferromagnet (FM) exchange-coupled to an antiferromagnet (AF), where the Curie temperature (T_C) of the FM is higher than the Neél temperature (T_N) of the AF. Nevertheless, new and interesting effects and features related to EB in systems where T_N is higher or close to T_C were already observed. The present work reports experimental results obtained on an AF/FM system with $T_C << T_N$, namely a magnetron sputtered (in a presence of magnetic field) bilayer of $NiO/Ni_{0.75}Cu_{0.25}$, already exhibiting EB in the as-deposited state.

Results

After the structural and magnetic characterization of the as-made film, it was cut into pieces that were divided into two groups. The first group of samples was submitted to thermal annealing. The samples of the second group were subjected to 50 keV He^+ irradiation at a current density of 100 nA/cm^2 at room temperature. Fluences of 510^{13}, 510^{14}, 110^{15}, and 510^{15} ions/cm^2 were used. During the ion bombardment, an external magnetic field, H_{IB}, with a magnitude of 5.5 kOe, was applied parallel or antiparallel to the original EB direction.

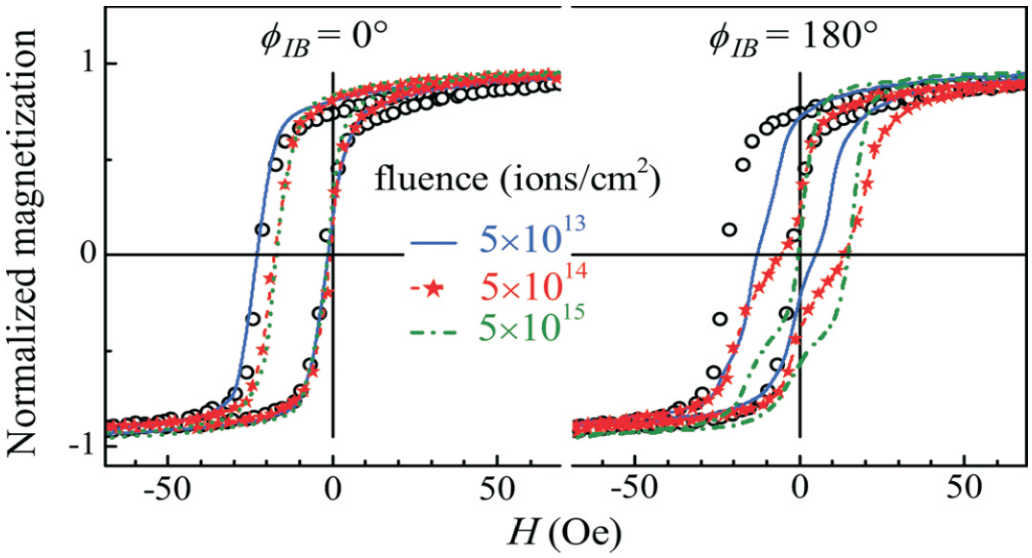

Figure 1. *Easy-axis loops of the as-made film (open symbols) and samples irradiated using different ion fluences (lines). (Left) H_{IB} parallel and (right) antiparallel to the original EB direction.*

Research outlook

Light-ion bombardment affects the NiO/NiCu bilayer in a rather different manner than the annealing. This technique could be a power tool to changing magnetic proprieties, specially the EB, of thin films. For example, in a forthcoming work (to be submitted for publication) we obtained that, by choosing the adequate fluence and/or ion type, one can attain a variation of more than one order of magnitude of the coercivity of IrMn/NiCu films.

Publications

[1] K. D. Sossmeier, L. G. Pereira, J. E. Schmidt, J. Geshev, *Exchange bias in a ferromagnet/antiferromagnet system with T_C<<T_N*, J. Appl. Phys. **109**, 083938 (2011).

[2] K. D. Sossmeier, L. G. Pereira, J. E. Schmidt, J. Geshev, *Tailoring the coercivity of unconventional AF/FM exchange-coupled bilayers* (unpublished).

The adhesion control of *Listeria monocytogenes* on food-processing surfaces by silver ion implantation

J. Lima

Introduction

Bacterial adhesion to a solid surface is a crucial step in the biofilm process. *Listeria monocytogenes* can adhere to food-processing surfaces, survive and grow over a wide range of environmental conditions such as refrigeration temperatures and consequently cause severe disease. Several strategies have been developed with the aim to decrease the adherence of bacteria to surfaces, namely the silver ion implantation on surfaces. The silver ions (Ag^{+1}) were implanted at AISI 304 and AISI 430 coupons (1 cm^{-2}). Adhesion assays with the bacterium *Listeria monocytogenes* were performed to evaluated if Ag^{+1} íons were capable to avoid cells adhesion on stainless steel surfaces.

Results

The results showed that the strain used was able to adhere to all materials. It was not found significant differences ($p > 0.05$) between the means of the *L. monocytogenes* adhered cells on the twelve surfaces studied. However, the highest mean value of adherence cells occurred to AISI 304 N° 4 (4.78 ± 0.32 log CFU.cm^{-2}) without silver ion implantation (wi) surface. Moreover, it was possible to observe that AISI 430 N° 8 with silver ion implantation (i) (4.29 ± 0.37 log CFU.cm^{-2}) and AISI 430 N° 4 wi (3.60 ± 0.31 log CFU.cm^{-2}) surfaces presentes the lowest means ($p < 0.05$). The contact time between microorganism and silver implantated stainless steel surfaces seems not to be enough to confer antimicrobial activity.

Research outlook

- Modification of food-processing surfaces (AISI 304 and AISI 430) with silver ion implantation (Ag^{+1});
- Control of *Listeria monocytogenes* cells adhesion.

Publications

[1] J. C. Lima, D. Schafer, et al., The adhesion control of *Listeria monocytogenes* on food-processing surfaces by silver ion implantation. **International Conference on Antimicrobial Research**, Oral presentation, Valladolid, Spain (2010).

Structural characterization of Pb nanoislands in SiO_2/Si interface synthesized by ion implantation through MEIS analysis

P. F. P. Fichtner

Introduction

The properties of a nanoparticle (NP) system strongly depend on their size, shape, number density and spatial order of the NP arrangement. It has been recently demonstrated that Medium Energy Ion Scattering (MEIS) can be used as a non destructive technique to provide accurate microstructure characterization of NP systems located at surface regions. In the present contribution we explore the MEIS potentiality to investigate buried 2-dimensional nanoparticle (NP) systems produced using a special on beam synthesis method [1]. As a model case system, we use a condensed planar arrangement of Pb NPs located under silica overlayers of distinct thicknesses. The MEIS measurements are compared to transmission electron microscopy (TEM) observations.

Results

The results obtained show that MEIS can be successfully used even if the nanostructures are not close to the surface. Multiple scattering effects are observed at lower scattering angles and must be accounted for. In this study, we demonstrate that SiO_2 overlayers with thickness about 45 nm already provide a good sensitivity for NP areal density and mean sizes, but the MEIS measurements are not sensitive for the details of the NP shape.

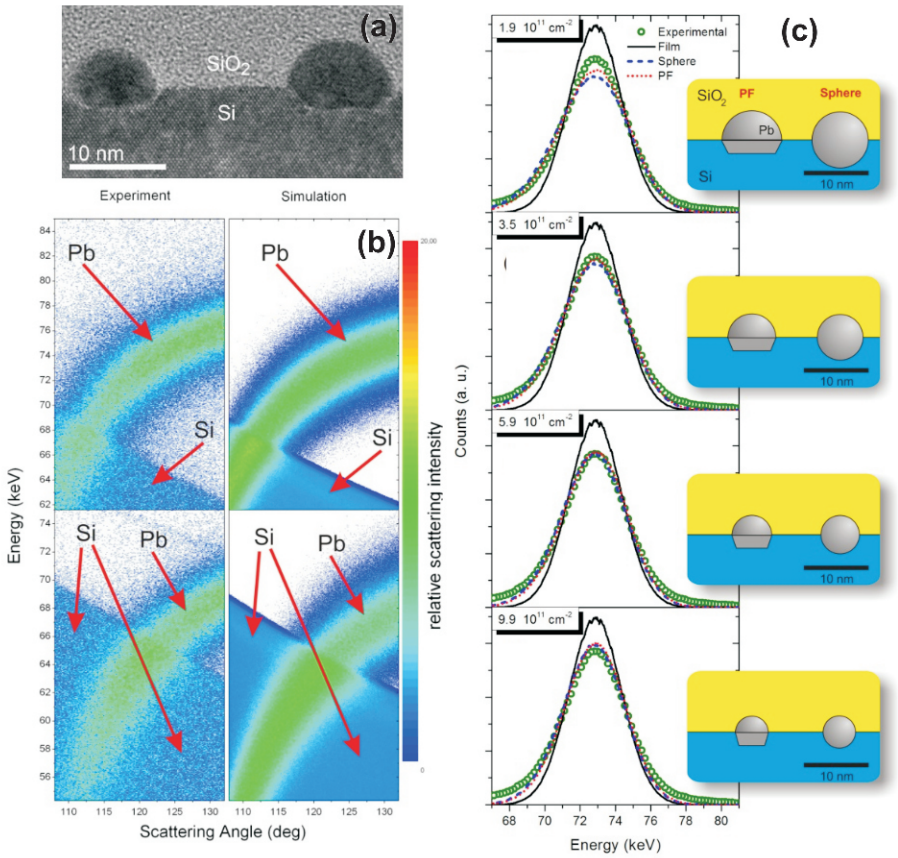

Figure 1 *(a) cross-section TEM micrograph from the Pb nanoparticles/ (b) measured and simulated MEIS spectra for overlayer thicknesses od 40 nm (top) and 60 nm (bottom); (c) Summed counts (120.6° to 132°) accounting for the overlayer thickness and distinct particle sizes and shapes. The best fit of the experimental data (open green circles) is obtained using the most realistic number density and NP sizes.*

Research outlook

In combination with TEM, the use of MEIS may be extended to determine stoichiometric variations in compound NP systems.

Publications

[1] F. P. Luce, F. Kremer, S. Reboh, Z. E. Fabrim, D. F. Sanchez, F. C. Zawislak, and P. F. P. Fichtner, J. Appl. Phys. **109**, 014320 (2011).

[2] D.F. Sanchez , F.P. Luce, Z.E. Fabrim, M.A. Sortica, P.F.P. Fichtner, P.L. Grande, Surface Science **605** 654–658 (2011).

Publications in peer reviewed articles

1) S. M. Shubeita, P. L. Grande, J. F. Dias, R. Garcia-Molina, C. D. Denton, I. Abril, ''Energy loss of swift H_2^+ and H_3^+ molecules in gols: Vicinage effects''. Physical Review B 83 (2011) 245423.

2) C. M. Viau, T. N. Guecheva, J. M. Cardone, M. L. Yoneama, J. F. Dias, C. Pungartnik, M. Brendel, J. Saffi, J. A. P. Henriques, ''The role of yeast low-affinity iron and zinc transport systems in stannous-induced toxicity''. FEBS Journal 278 (2011) 430.

3) C. E. I. dos Santos, S. M. Shubeita, L. Amaral, P. L. Grande, J. F. Dias, ''Depth profiling techniques: how PIXE compares to NRP and MEIS?''. X-Ray Spectrometry 40 (2011) 157.

4) E. D. Cantero, C. C. Montanari, M. Behar, R. C. Fadanelli, G. H. Lantschner, J. E. Miraglia, and N. R. Arista, ''Experimental and theoretical study of the energy loss of C and O in Zn''. Physical Review A 84 (2011) 014902.

5) M. Behar, R. C. Fadanelli, I. Abril, R. Garcia-Molina, and L. C. C. Nagamine, ''Energy-loss straggling study of proton and alpha-particle beams incident onto ZrO2 and Al2O3 films''. The European Physical Journal D 64 (2011) 297.

6) Mirella Peña-Icart, Margarita E. Villanueva Tagle, Carlos Alonso-Hernandez, Joelis Rodriguez Hernandez, Moni Behar, Mario S. Pomares Alfonso, ''Comparative study for digestion Methos ESPAA for Cu, Ni, and Pb contamination assesment in marine sediments''. Marine Enviroment Research Vol 72, 1,2 (2011) 6611.

7) F. L. Bregolin, M. Behar, U. S. Sias, E. C. Moreira, ''Structural and photoluminiscence properties of Si nanoclusters obtained by ion implantation into Si3N4 films''. Journal of Luminiscence, 131 (2011) 2377-2381.

8) G.V. Soares, C. Krug, L. Miotti, K.P. Bastos, G. Lucovsky, I.J.R. Baumvol, and C. Radtke, ''Intermixing between HfO_2 and GeO_2 films deposited on Ge(001) and Si(001): Role of the substrate.'' Applied Physics Letters, v. 98 (2011) p. 131912.

9) Strapasson, G. ; Badin, P.C. ; Soares, G.V. ; Machado, G. ; Figueroa, C.A ; Hubler, R. ; Gasparin, A.L. ; Baumvol, I.J.R. ; C.Aguzzoli, ; Tentardini, E.K. . ''Structure, composition, and mechanical characterization of dc sputtered TiN-MoS2 nanocomposite thin films.'' Surface & Coatings Technology, v. 205 (2011) p. 3810-3815.

10) FILLA, J. ; AGUZZOLI, C. ; SONDA, V. ; Farias, M.C.M. ; Soares, G.V. ; Baumvol, I.J.R. ; Figueroa, C.A. . ''Nanoscale friction of partially oxidized silicon nitride thin films.'' Surface & Coatings Technology (2011) p. 4528.

11) Pitthan, Eduardo ; Corrêa, Silma A. ; Palmieri, Rodrigo ; Soares, Gabriel V. ; Boudinov, Henri I. ; Stedile, Fernanda C. . ''Effect of Reoxidations and Thermal Treatments with Hydrogen Peroxide in the SiO2/SiC Interfacial Region.'' Electrochemical and Solid-State Letters, v. 14 (2011) p. H368.

12) R. Brambilla, C. Radtke, F.C. Stedile, J.H.Z. dos Santos, M.S.L. Miranda, ''Metallocene catalyst supported on silica–magnesia xerogels for ethylene polymerization'', Applied Catalysis A: General v. 382 (2010) p. 106.

13) Crespi, Ângela E. ; da Costa, Marcelo E.H. Maia ; Figueroa, Carlos A. ; Dotto, Marta E.R. ; Kauling, Alan P. ; Soares, Gabriel V. ; Baumvol, Israel J.R. ; Giacomelli, Cristiano . ''Carbon nitride film deposition by active screen plasma nitriding.'' Materials Letters (General ed.), v. 65 (2011) p. 2985-2988.

14) D. Schafer, P. L. Grande, L. G. Pereira, and J. Geshev, ''Ion irradiation effects on the exchange bias in IrMn/Co films'' , Journal of Applied Physics 109 (2011) 023905.

15) D.F. Sanchez, F.P. Luce, Z.E. Fabrim, M.A. Sortica, P.F.P. Fichtner, P.L. Grande, ''Structural characterization of Pb nanoislands in SiO2/Si interface synthesized by ion implantation through MEIS analysis'', Surface Science 605 (2011) 654–658.

16) H. Hijazi, L.S. Farenzena, H. Rothard, Ph. Boduch, P.L. Grande, and E.F. da Silveira,'' Cluster ion emission from LiF induced by MeV Nq+ projectiles and ^{252}Cf fission fragments'', Eur. Phys. J. D 63 (2011) 391–400.

17) G. Machado, A. F. Feil, P. Migowski, L. Rossi, M. Giovanela, J. da S. Crespo, L. Miotti, M. A. Sortica, P. L. Grande, M. B. Pereira and R. R. B. Correia, ''Structural control of gold nanoparticles self-assemblies by layer-by-layer process'', Nanoscale, 3 (2011) 1717.

18) G. Schiwietz, K. Czerski, P.L. Grande , V. Koteski , F. Staufenbiel, ''Ultrafast band-structure variations induced by fast Au ions in BeO'', Nuclear Instruments and Methods in Physics Research B 26 (2011) 959–963.

19) G. Schiwietz and P.L. Grande, ''Introducing electron capture into the unitary-convolution-approximation energy-loss theory at low velocities'', Physical Review A 84 (2011) 052703.

20) A. J. Window, A. Hentz, A., D. C. Sheppard, G. S. Parkinson, H. Niehus, D. Ahlbehrendt, T. C. Q. Noakes, P. Bailey, D. P. Woodruff, ''V2O3(0001) Surface Termination: Phase Equilibrium'', Physical Review Letters, 107 (2011) 016105.

21) D. C. Sheppard, G. S. Parkinson, A. Hentz, A. J. Window, P. D. Quinn, D. P. Woodruff, P. Bailey, T. C. Q. Noakes, ''Medium energy ion scattering investigation of methylthiolate-induced modification of the Au(111) surface'', Surface Science, 605 (2011) 138-145.

22) T. C. Q. Noakes, P. Bailey, C. F. McConville, M. Draxler, M. Walker, M. G. Brown, A. Hentz, D. P. Woodruff, T. A. Lograsso, A. R. Ross, J. A. Smerdon, L. Leung, R. McGrath, ''Two- and three-dimensional growth of Bi on i-Al-Pd-Mn studied using medium-energy ion scattering'', Physical Review B, 82 (2010) 195418.

23) A. J. Window, A. J., A. Hentz, D. C. Sheppard, G. S. Parkinson, D. P. Woodruff, T. C. Q. Noakes, P. Bailey, ''Silver sulphide growth on Ag(111): A medium energy ion scattering study'', Surface Science, 604 (2010) 1254-1260.

24) D. C. Sheppard, G. S. Parkinson, A. Hentz, P. D. Quinn, M. A. Munoz-Marquez, D. P. Woodruff, P. Bailey, T. C. Q. Noakes, ''Surface relaxation in Cu(410)-O: A medium energy ion scattering study'', Surface Science, 604 (2010) 788-796.

25) E. L. da Rocha, C. R. da Cunha, ''The transition from fracton to phonon states in a Sierpinski triangle lattice'', Chaos, Solitons & Fractals, 44 (2011) 241.

26) J. da Silva Jr., C. R. da Cunha, F. L. de Carvalho, U. P. Rodrigues Filho, P. R. Oliveira, M. A. Segatto Silva, ''Obtaining high purity silica from rice hulls'', Quimica Nova, 33 (2010) 794.

27) M. K. Santala, V. Radmilovic, R. Giulian, M. C. Ridgway, R. Gronsky, A. M. Glaeser, ''The orientation and morphology of platinum precipitates in sapphire'', Acta Materialia, 59 (2011) 4761.

28) D. J. Sprouster, R. Giulian, L. L. Araujo, P. Kluth, B. Johannessen, N. Kirby, M. C. Ridgway, ''Formation and structural characterization of Ni nanoparticles embedded in SiO(2)'', Journal of Applied Physics, 109 (2011) 113517.

29) D. J. Sprouster, R. Giulian, L. L. Araujo, P. Kluth, B. Johannessen, D. J. Cookson, M. C. Ridgway, ''Swift heavy-ion irradiation-induced shape and structural transformation in cobalt nanoparticles'', Journal of Applied Physics, 109 (2011) 113504.

30) H. Amekura, N. Ishikawa, N. Okubo, M. C. Ridgway, R. Giulian, K. Mitsuishi, Y. Nakayama, C. Buchal, S. Mantl, N. Kishimoto, ''Zn nanoparticles irradiated with swift heavy ions at low fluences: Optically-detected shape elongation induced by nonoverlapping ion tracks'', Physical Review B, 83 (2011) 205401.

31) R. Giulian, L. L. Araujo, P. Kluth, D. J. Sprouster, C. S. Schnohr, A. P. Byrne, M. C. Ridgway, ''Swift heavy ion irradiation of Pt nanocrystals: II. Structural changes and H desorption'', Journal of Physics D - Applied Physics, 44 (2011) 155402.

32) R. Giulian, L. L. Araujo, P. Kluth, D. J. Sprouster, C. S. Schnohr, A. P. Byrne, M. C. Ridgway, ''Swift heavy ion irradiation of Pt nanocrystals: I. shape transformation and dissolution'', Journal of Physics D - Applied Physics, 44 (2011) 155401.

33) M. C. Ridgway, R. Giulian, D. J. Sprouster, P. Kluth, L. L. Araujo, D. J. Llewellyn, A. P. Byrne, F. Kremer, P. F. P. Fichtner, G. Rizza, H. Amekura, M. Toulemonde, ''Role of thermodynamics in the shape transformation of embedded metal nanoparticles induced by swift heavy-ion irradiation'', Physical Review Letters, 106 (2011) 095505.

34) B. Afra, M. Lang, M. D. Rodriguez, J. Zhang, R. Giulian, N. Kirby, R. C. Ewing, C. Trautmann, M. Toulemonde, P. Kluth, ''Annealing kinetics of latent particle tracks in Durango apatite'', Physical Review B, 83 (2011) 064116.

35) T. Steinbach, C. S. Schnohr, P. Kluth, R. Giulian, L. L. Araujo, D. J. Sprouster, M. C. Ridgway, W. Wesch, ''Influence of electronic energy deposition on the structural modification of swift heavy-ion-irradiated amorphous germanium layers'', Physical Review B, 83 (2011) 054113.

36) E. Granado, L. Mendonça-Ferreira, F. Garcia, G. de M. Azevedo, G. Fabbris, E. M. Bittar, C. Adriano, T. M. Garitezi, P. F. S. Rosa, L. F. Bufaiçal, M. A. Avila, H. Terashita, P. G. Pagliuso, ''Pressure and chemical substitution effects in the local atomic structure of $BaFe_2As_2$'', Physical Review B, 83 (2011) 184508.

37) X. Liu, J. Kjelstrup-Hansen, H. Boudinov, H. G. Rubahn, ''Charge-carrier injection assisted by space-charge field in AC-driven organic light-emitting transistors'', Organic Electronics, 12 (2011) 1724.

38) A. V. P. Coelho, M. C. Adam, H. Boudinov, ''Distinguishing bulk traps and interface states in deep-level transient spectroscopy'', Journal of Physics. D, Applied Physics, 44 (2011) 305303.

39) Luce, F. P. ; Kremer, F. ; Reboh, S. ; Fabrim, Z. E. ; Sanchez, D. F. ; Zawislak, F. C. ; Fichtner, P. F. P.. ''Aging effects on the nucleation of Pb nanoparticles in silica.'' Journal of Applied Physics, v. 109 (2011) p. 014320.

40) C.T. Dominguez, R.L. Maltez, R.M.S. dos Reis, L.S.A. de Melo, C.B. de Araujo, A.S.L. Gomes, ''Dependence of random laser emission on silver nanoparticle density in PMMA films containing rhodamine 6G '',Journal of the Optical Society of America B - Optical Physics, 28 (2011) 1118.

41) A. F. Feil, P. Migowski, J. Dupont, L. Amaral, S. R. Teixeira, ''Nanoporous Aluminum Oxide Thin Films on Si Substrate: Structural Changes as a Function of Interfacial Stress''. Journal of Physical Chemistry C, 115 (2011) 7621-7627.

42) K. D. Sossmeier, L. G. Pereira, J. E. Schmidt, J. Geshev, “Exchange bias in a ferromagnet/antiferromagnet system with TC << TN”, Journal of Applied Physics 109 (2011) 083938.

43) Corujeira Gallo, Santiago; Crespi, Ângela E.; Cemin, Felipe; Figueroa, Carlos A.; Baumvol, Israel J. R. . ''Electrostatically Confined Plasma in Segmented Hollow Cathode Geometries for Surface Engineering''. IEEE Transactions on Plasma Science, 66 (2011) 714.

44) Roman, Daiane; Bernardi, Juliane; Amorim, Cintia L.G. de; de Souza, Fernando S.; Spinelli, Almir; Giacomelli, Cristiano; Figueroa, Carlos A.; Baumvol, Israel J.R.; Basso, Rodrigo L.O. . ''Effect of deposition temperature on microstructure and corrosion resistance of ZrN thin films deposited by DC reactive magnetron sputtering.'' Materials Chemistry and Physics , 167 (2011) 3472.

45) Trentin, Danielle da Silva; Giordani, Raquel Brandt; Zimmer, Karine Rigon; da Silva, Alexandre Gomes; da Silva, Márcia Vanusa; Correia, Maria Tereza dos Santos; Baumvol, Israel Jacob Rabin; Macedo, Alexandre José. ''Potential of medicinal plants from the Brazilian semi-arid region (Caatinga) against Staphylococcus epidermidis planktonic and biofilm lifestyles.'' Journal of Ethnopharmacology, 106 (2011) 759.

46) Rovani, A.C.; Crespi, A.E.; Sonda, V.; Cemin, F.; Echeverrigaray, F.G.; Amorim, C.L.G.; Basso, R.L.O.; Baumvol, I.J.R.; Figueroa, C.A. . ''Plasma post-oxidation mechanisms of nitrided ferrous alloys.'' Surface & Coatings Technology, 205 (2011) 3422-3428.

47) Thomaz, R. S.; Souza, C. T.; Papaléo, R. M. ''Influence of light-ion irradiation on the heavy-ion track etching of polycarbonate.'' Applied Physics. A, Materials Science & Processing, v. 104 (2011) p. 1223-1227.

48) Maniks, J.; Manika, I.; Grants, R.; Zabels, R.; SCHWARTZ, K.; Sorokin, M.; Papaleo, R. M. ''Nanostructuring and hardening of LiF crystals irradiated with 3-15 MeV Au ions.'' Applied Physics. A, Materials Science & Processing, v. 104 (2011) p. 1121-1128.

49) Siles, Pablo F. ; Archanjo, B. S. ; Baptista, D. L. ; Pimentel, V. L. ; Joshua, J.; Neves, B. R. A. ; Medeiros-Ribeiro, G. ''Nanoscale lateral switchable rectifiers fabricated by local anodic oxidation.'' Journal of Applied Physics, v. 110 (2011) p. 024511, 2011.

50) Almeida, F. A. ; Oliveira, F. J. ; Silva, R. F. ; Baptista, D. L. ; Peripolli, S. B. ; Achete, C. A. ''High resolution study of the strong diamond/silicon nitride interface.'' Applied Physics Letters, v. 98 (2011) p. 171913.

51) D. M. Schaefer, P. F. P. Fichtner, M. Carara, L. F. Schelp and L. S. Dorneles, ''Dielectric breakdown in AlOx tunnelling barriers'', J. Phys. D: Appl. Phys. 44 (2011) 135403 (5pp).

52) S. Reboh, A.A.D. de Mattos, F. Schaurich, P.F.P. Fichtner, M.F. Beaufortd and J.F. Barbot, ''The mechanisms of surface exfoliation in H and He implanted Si crystals'', Scripta Materialia 65 (2011) 1045–1048.

53) Flavia P. Luce, Felipe Kremer, Dario F. Sanchez, Zacarias E. Fabrim, Shay Reboh, Fernando C. Zawislak and Paulo F. P. Fichtner, ''Formation of dense and aligned planar arrangements of Pb nanoparticles at silica/silicon interfaces'', Mater. Res. Soc. Symp. Proc. Vol. 1308 (2011).

Conference proceedings

1) C. Radtke, N.M. Bom, G.V. soares, C. Krug, I.J.R. Baumvol, ''Interaction of Aluminum Oxide with Germanium during Thermal Annealing in Ar, N_2/H_2, O_2, or H_2O.'' In: 220th ECS Meeting and Electrochemical Energy Summit, 2011, Boston. ECS Transactions. Pennington : The Electrochemical Society, 2011. v. 41. p. 21-28.

2) D. H. C. de Souza, C. R. da Cunha, ''A possible tool for fabricating electronic devices through local electrochemistry'' In: 25th Symposium on Microelectronics Technology and Devices, 2010, São Paulo. ECS Transactions. Pennington : The Electrochemical Society, 2010. v.31, p.149-154.

3) Sombrio, G. ; Mattos, A. E. P. ; Franzen, P.L. ; Pereira, M. B. ; Boudinov, H., ''Photoluminescence in Non-Stoichiometric Silicon Nitride Films Obtained by Reactive Sputtering'' In: 26th Symposium on Microelectronics Technology and Devices (SBMicro 2011), 2011, Joao Pessoa. Microelectronics Technology and Devices - SBMicro 2011, 2011. v. 39. p. 315-320.

4) Mattos, A. E. P. ; Sombrio, G. ; Franzen, P.L. ; Pereira, M. B. ; Boudinov, H., ''Si Nanocrystals Embedded in SiO2 Produced by Reactive Sputtering for Light Emission'' In: 26th Symposium on Microelectronics Technology and Devices (SBMicro 2011), 2011, João Pessoa. Microelectronics Technology and Devices - SBMicro 2011, 2011. v. 39. p. 103-108.

5) PALMIERI, Rodrigo ; RADTKE, C ; Boudinov, H. ; SILVA JR, Eronides F. da . ''Effect of H2O2 in passivation of n- and p-type 4H-SiC surfaces.'' In: 13th ICFSI International Conference on the Formation of Semiconductor Interfaces, 2011, Praga. 13th ICFSI, 2011.

6) PALMIERI, Rodrigo ; Boudinov, H. ; RADTKE, C ; SILVA JR, Eronides F. da . ''Effects of oxidation temperature and substrate doping on the properties of thermal oxide layer and interface of SiO2/4H-SiC.'' In: ACSIN11, 11th International Conference on Atomically Controlled Surfaces, Interfaces, and Nanostructures, 2011, St. Petersburg, Russia. ACSIN_2011, 2011.

7) Boudinov, H. ; M. Boff . ''Quantum Hall Effect as an Electrical Resistance Standard.'' In: 26th Symposium on Microelectronics Technology and Devices - SBMicro 2011, 2011, Joao Pessoa. Microelectronics Technology and Devices - SBMicro 2011, 2011.

8) Reis R.M.S dos ; MALTEZ, R.L. ; Boudinov, H. . ''Structural characterization of $Si_{1-x}C_x$ nanolayers synthesized by C implantation into SiO_2/Si.'' In: 26th Symposium on Microelectronics Technology and Devices - SBMicro 2011, 2011, Joao Pessoa. Microelectronics Technology and Devices - SBMicro 2011, 2011.

9) M. Adam ; COELHO, A. V. P. ; M.B. Pereira ; Boudinov, H. . ''Sputtered Silicon Nitride Thin Films for Non-Volatile Memory Applications.'' In: 26th Symposium on Microelectronics Technology and Devices - SBMicro 2011, 2011, Joao Pessoa. Microelectronics Technology and Devices - SBMicro 2011, 2011.

10) Cauduro, A. L. F. ; Pesenti, G. C. ; Oliveira, J. W. L. ; Zawislak, F. C. ; Boudinov, H. I. ; Baptista, D. L. ''Zinc oxide nanowires semiconductors for nanosensing applications.'' In: 1st Brazilian German Workshop on Micro- And Nano-Electronics - BGME, 2010, Porto Alegre.

Patent

Method of fabricating gallium nitride (GaN) based substrate of semiconductor device e.g. LED, involves annealing substrate such that bubbles of implanted ion species are formed at appropriate distance from buffer/silicon interface.

Patent Number(s): US2010046567-A1 ; US8008181-B2
Inventor(s): LILIENTAL-WEBER Z., MALTEZ R. L., MORKOC H., XIE J.
Patent Assignee Name(s) and Code(s): UNIV CALIFORNIA(REGC-C)
Derwent Primary Accession Number: 2010-C16184 [57]
Date Issued: 30-Aug-2011

Oral contributions and invited talks

1. J. F. Dias: 12nd International Conference on Particle Induced X-Ray Emission and Its Analytical Applications (PIXE 12), Guilford, UK (2010). Invited talk.

2. J. F. Dias: 7th International Symposium on Bio-PIXE (Bio-PIXE 7), Sendai, Japan (2011). Invited talk.

3. M. Behar : 16 International Conference on Radiation Effects on Insulators, Peking, China (2011). Invited talk.

4. M. Behar: Fourth International Conference on Radiation Effects on the Matter, Padova, Italy 2011. Invited talk.

5. C. Radtke: 220th ECS Meeting and Electrochemical Energy Summit, Boston, USA (2011). Oral presentation.

6. G.V.Soares: 20th International Conference on Ion Beam Analysis, Itapema, Brazil (2011). Oral presentation.

7. G.V.Soares: Materials Research Society Spring Meeting 2011, San Francisco, USA (2011). Oral presentation.

8. G.V.Soares: X Brazilian MRS Meeting, Gramado, Brazil (2011). Oral presentation.

9. S.A. Corrêa: 20th International Conference on Ion Beam Analysis, Itapema, SC (2011). Oral presentation.

10. F.C. Stedile: International Conference on Silicon Carbide and Related Materials, Cleveland, OH, USA (2011). Invited talk.

11. P. L. Grande : 20th International Conference on Ion Solid Interactions, Zvenigrod, Russia (2011). Invited talk.

12. P.L. Grande : X SBPmat.X Brazilian Material Society, Gramado (2011). Invited talk.

13. P.L. Grande : IV Brazilan school on magnetism, Ouro Preto (2011). Invited talk.

14. A. Hentz: High-Resolution Depth Profiling 6, Paris (2011). Oral presentation.

15. H. Boudinov: Microelectronics Technology and Devices Meeting SBMICRO 2011, João Pessoa, Brazil. Oral presentation.

16. M. Adam: Microelectronics Technology and Devices Meeting SBMICRO 2011, João Pessoa, Brazil. Oral presentation.

17. A.E.P. de Mattos: Microelectronics Technology and Devices Meeting SBMICRO 2011, João Pessoa, Brazil. Oral presentation.

18. R.M.S. dos Reis: Microelectronics Technology and Devices Meeting SBMICRO 2011, João Pessoa, Brazil. Oral presentation.

19. G. Sombrio: Microelectronics Technology and Devices Meeting SBMICRO 2011, João Pessoa, Brazil. Oral presentation.

20. M. A. Sortica: High-Resolution Depth Profiling 6, Paris (2011). Oral presentation.

21. M. A. Sortica: V Encuentro Sud-Americano de Colisiones Inelásticas en la Materia, Valparaíso - Chile (2010). Oral presentation.

22. D. F. Sanchez: High-Resolution Depth Profiling 6, Paris (2011). Oral presentation.

23. D. F. Sanchez: 21ª Reunião Anual de Usuários do LNLS, Campinas (2011). Oral presentation.

24. D. F. Sanchez: V Encuentro Sud-Americano de Colisiones Inelásticas en la Materia, Valparaíso - Chile (2010). Oral presentation.

25. G. Azevedo: X SBPmat X Brazilian Materials Society Meeting, Gramado (2011). Oral presentation.

26. R. L. Maltez: EMRS 2011 Spring meeting - Symposium B, Nice, France. Oral presentation.

27. Papaléo, R. M. 20th International Conference on Ion Beam Analysis (2011). Oral presentation.

28. D.L. Baptista: XXIII Congresso da Sociedade Brasileira de Microscopia e Microanálise, Búzios (2011). Oral presentation.

29. D.L. Baptista: X Brazilian MRS Meeting, Gramado (2011). Oral presentation.

30. P. F. P. Fichtner: XXIII Congresso da Sociedade Brasileira de Microscopia e Microanálise, Búzios (2011). Oral presentation.

31. P. F. P. Fichtner: 20th International Conference on Ion Beam Analysis, Itapema-SC (2011). Oral presentation.

32. P. F. P. Fichtner: Technical Meeting on Radiation Induced Defects in Semiconductors and Insulators (F1-TM-40764), Vienna (2011). Oral presentation.

33. P. F. P. Fichtner: Workshop on FE-SEM and Energy Filtered TEM, Campinas-SP (2011). Invited talk.

Books and book chapters

1)Propridades eletro-oticas e nanoestruturas de germanio produzidas por implantação ionica a quente, F. L. Bregolin, U. s. Sias, M. Behar, E. C. Moreira em Topicos em Nanociencia e Nanotecnologia, Volume II,Pag 63, Editoria UFRGS 2011.

2) Nanocristais semicondutores, C. Krug e C. Radtke em Topicos em Nanociencia e Nanotecnologia, Volume II,Pag 165, Editoria UFRGS 2011.

Supervision of theses and dissertations

1. Nicolau Molina Bom. Dissertation (2011). Supervisor: C. Radtke.

2. Luciana Valgas de Souza. Dissertation (2010). Supervisor: C. R. da Cunha.

3. Daniel Henrique de Souza. Dissertation (2010). Supervisor: C. R. da Cunha.

4. Iuri Stefani Brandt. Dissertation (2010). Supervisor: C. R. da Cunha.

5. Daniel Travessini. Dissertation (2010). Supervisor: C. R. da Cunha.

6. Milton André Tumelero. Dissertation (2010). Supervisor: C. R. da Cunha.

7. Genevieve Kreibich Pinheiro. Dissertation (2010). Supervisor: C. R. da Cunha.

8. Edroaldo Lummertz da Rocha. Dissertation (2010). Supervisor: C. R. da Cunha.

9. Denize Maria Hoffmeister. Dissertation (2010). Supervisor: C. R. da Cunha.

10. Antonio Augusto Malfatti Gasperini. PhD Thesis - UNICAMP (2011). Supervisor: Gustavo Azevedo.

11. Eliasibe Luis de Souza. Dissertation (2011). Supervisor: H. Boudinov.

12. Carla Eliete Iochims dos Santos. PhD Thesis (2011). Supervisor: Johnny Ferraz Dias

13. Zacarias E. Fabrim. Dissertation (2011). Supervisor: Paulo F. P. Fichtner.

Members in international commitees and in editorial boards of scientific journals

• Fernanda C. Stedile - Member of the international committee of the International Conference on Ion Beam Analysis

• Pedro L. Grande - Member of the international committee of the International Conference on Ion Beam Analysis

• Pedro L. Grande - Editorial Board Nucl. Instr. and Methods B

• Johnny Ferraz Dias - Member of the International Committee of the International Conference on Particle-Induced X-ray Emission

• Johnny Ferraz Dias - Member of the International Committee of the International Symposium on BioPIXE

• Moni Behar - Member of the International Committee of the Radiation Effects in Insulators.

• Moni Behar - Member of the International Comittee of Ion Beam Modification of the Materials

• Moni Behar - Member of International Committee of Radiation Effects on the Materials.

• Moni Behar - Member of the International Committee of Colisiones Inelasticas na Materia

Seminars

Fernando Pablo Cometto
Departamento de Físicoquímica, INFIQC, Universidad Nacional de Córdoba, Argentina
Reaction mechanisms, synthesis and assembly of nanoparticles and nanostructures

Israel Ayala
Beneq (fabricante de equipamentos para ALD)
Fundamentals and applications of Atomic Layer Deposition

Dietmar Fink
Prof. Visitante Lab. de Implant.
The use of ion irradiation for biotechnology

Dae Won Moon
Korea Research Institute of Standards and Science (KRISS)
Nano bio imaging / MEIS in KRISS

Jerome Leveneur
Geological and Nuclear Science - National Isotope Center - New Zealand
Synthesis and characterization of surface magnetic nanoclusters

Leandro Langie
IF-UFRGS
Saboneteando na Australia - six years down under

Adriano Feil
IF-UFRGS
Formação de óxidos nanoestruturados pelo processo de anodização: Conceitos básicos e aplicações

Raquel Giulian
IF-UFRGS
Modificação de nanopartículas por feixes de íons (Shape transformation of embedded nanoparticles using ion irradiation)

Cilâine Teixeira
IF-UFRGS
Caracterizaçao de sistemas formados por surfactantes por SAXS

Flavia P. Luce
PG - Física
Síntese de nanopartículas de Pb e PbSe em matrizes de SiO2/Si via implantação iônica (pré apresentação exame de qualificação)

Dario Sanchez & Mauricio Sortica
apresentações orais na HRDP6 - Paris junho 2011
Análise de nanoestruturas via MEIS: a) sistemas enterrados (Dario) e b) sistemas compostos (Maurício)

Fernando Mendonza
FEI - USA
Microscópios Eletrônicos de Varredura FEG de alta resolução
sala de seminários do Centro de Microscopia Eletrônica

Zacarias E. Fabrim
Lab. de Implantação
Ion Beam Synthesis of PbSe and CdSe nanocrystals in thin film heterostructures

Yan Levin
IF-UFRGS
Ions at the air-water interface, surface tensions, surface potential and Hofmeister series of electrolyte solutions

Rita M. de Almeida
IF-UFRGS
Genoma e sua expressão: muitos dados e pouca informação.

Gilberto Madeiros Ribeiro
HP-USA
Understanding memristors: using physics, materials science and information theory to engineer a new class of non-volatile storage

Paulo Pureur
IF-UFRGS
Contribuição da Quiralidade ao Efeito Hall de Sistemas Magnéticos Desordenados

Partners/Projects (Universities, Research Institutes and Companies)

PRONEX

INCT-INES

Nanobiotec

INCT-Namitec

PNPD-CAPES

R-NANO

PETROBRAS

CAPES/MES, Cuba 2009-2011

Capes/Probral, Germany 2009-2011.

Capes/Mincyt 2010-2011

École Polytechnique de Nancy, CAPES – Brafitec.

Pontifícia Universidade Católica - RJ, INCT e PROCAD.

UFSC

UFPR.

Funding Agencies

PRONEX

Petróleo Brasileiro S.A.

Laboratório de Implantação Iônica

Ion Implantation Laboratory
Institute of Physics
Federal University of Rio Grande do Sul – UFRGS

Av. Bento Gonçalves, 9500
91501 - 970 Porto Alegre, RS Brazil
Phone: +55-51-3308-7004, Fax: +55-51-3308-7296
http://www.implantador.if.ufrgs.br

Ion Implantation Laboratory
Institute of Physics - UFRGS
Porto Alegre
Brazil